Electronic supplementary information (ESI)

Fine tuning catalytic and sorption properties of metal-organic frameworks *via in situ* ligand exchange

Peng Wang,[a] Kai Chen,[a] Qing Liu,[a] Huai-Wei Wang,[a] Mohammad Azam,[b] Saud I Al-Resayes,[b] Yi Lu*[a] and Wei-Yin Sun*[a]

Fig.S1-S6 Ellipsoids drawing of **1-6**

Fig.S7-S9 PXRD patterns of **1-6**

Fig.S10-S15 ^{1}H-NMR spectra of digested **1-6**

Fig.S16 Electron density maps (F_o) obtained by time-dependent X-ray diffraction

Fig.S17-S22 TGA curves of **1–6**

Fig.S23-S28 FT-IR spectra of **1-6**

Fig.S29-S41 sorption properties of **1-6**

Fig.S42 PXRD patterns for MOF **6** before and after the reaction

Table S1. Crystal data and structure refinements for **1 - 6**

Table S2. Selected bond lengths (Å) and angles (°) for **1** – **6**

Table S3. Unit cell, BET and Langmuir surface areas, pore volumes, porosities and Q_{st}^{o} for the isoreticular MOFs

Table S4. Knoevenagel condensation of different benzaldehyde with ethyl cyanoacetate

Experimental:

Materials and Methods

Synthesis of **1-6**

General Procedures

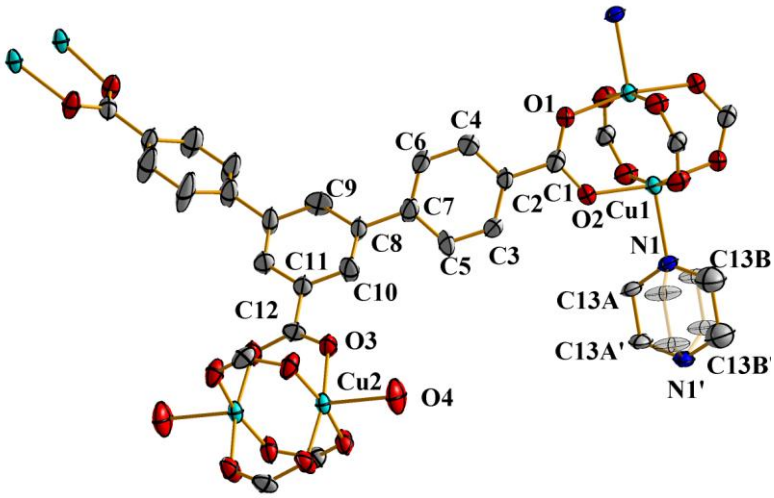

Fig. S1. Coordination environment of Cu(II) in **1** with ellipsoids drawn at the 30% probability level. Hydrogen atoms and free solvents are omitted for clarity.

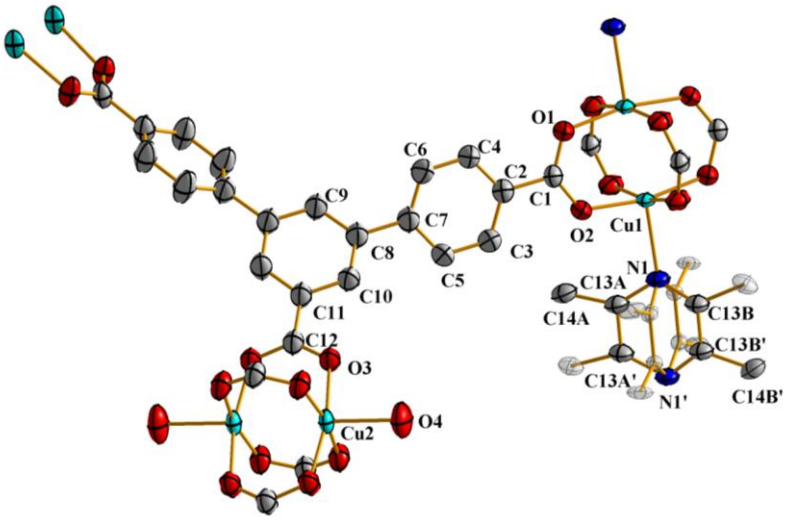

Fig. S2. Coordination environment of Cu(II) in **2** with ellipsoids drawn at the 30% probability level. Hydrogen atoms and free solvents are omitted for clarity.

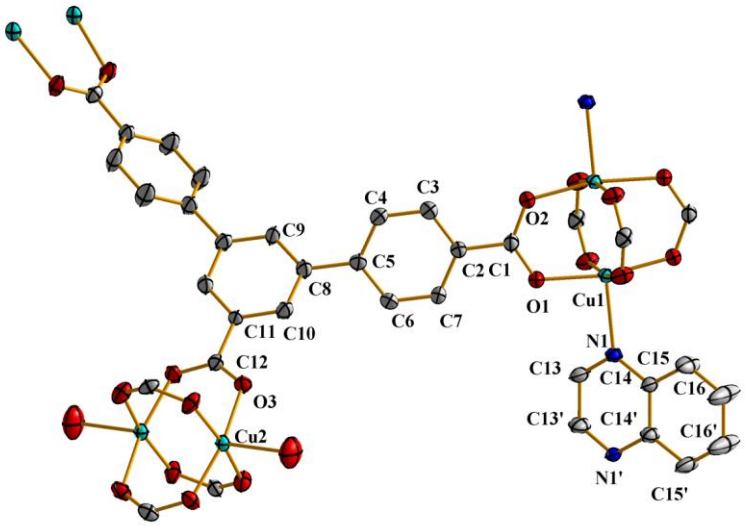

Fig. S3. Coordination environment of Cu(II) in **3** with ellipsoids drawn at the 30% probability level. Hydrogen atoms and free solvents are omitted for clarity.

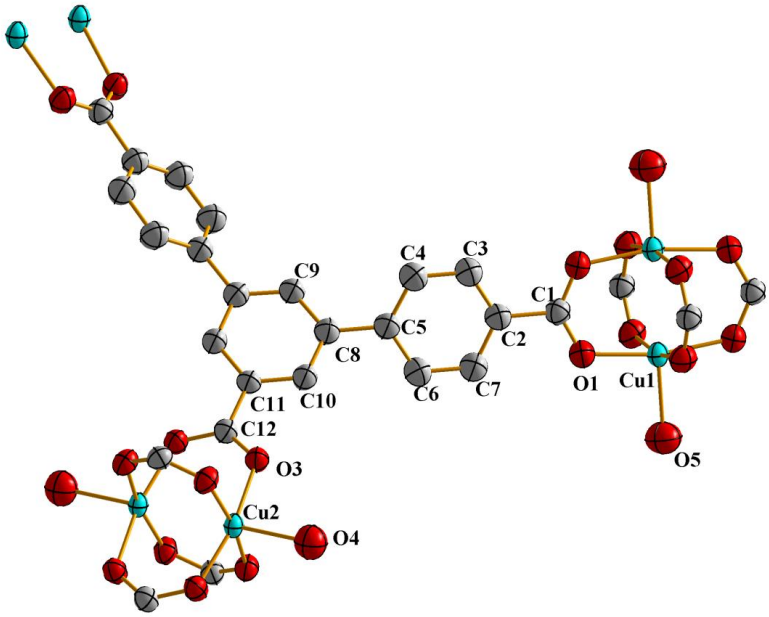

Fig. S4. Coordination environment of Cu(II) in **4** with ellipsoids drawn at the 30% probability level. Hydrogen atoms and free solvents are omitted for clarity.

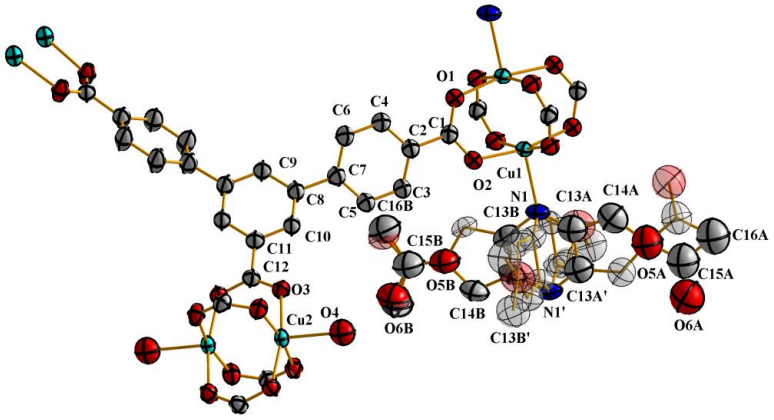

Fig. S5. Coordination environment of Cu(II) in **5** with ellipsoids drawn at the 30% probability level. Hydrogen atoms and free solvents are omitted for clarity.

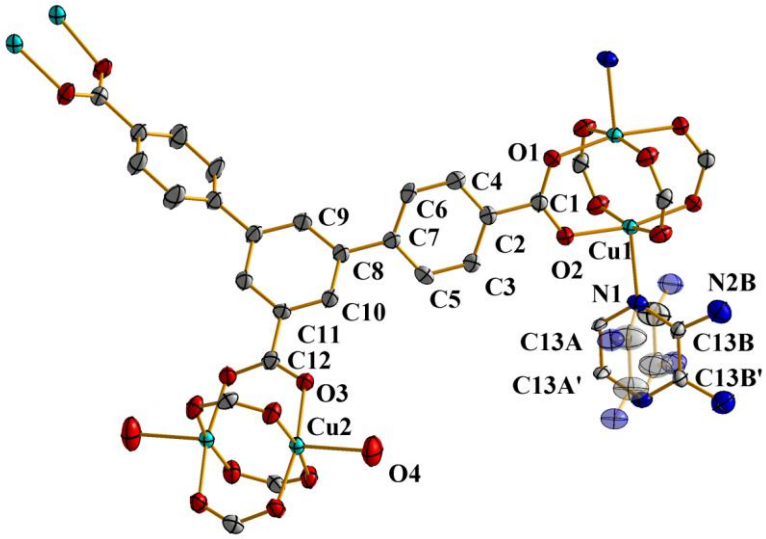

Fig. S6. Coordination environment of Cu(II) in **6** with ellipsoids drawn at the 30% probability level. Hydrogen atoms and free solvents are omitted for clarity.

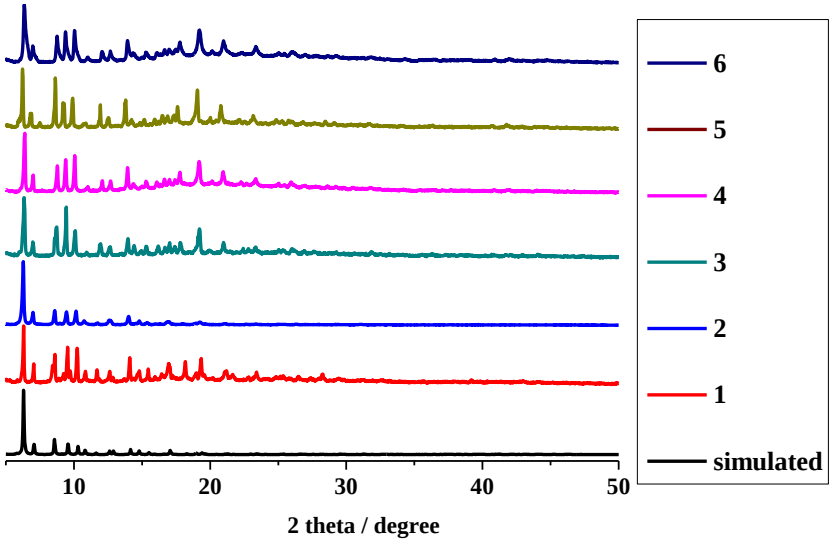

(a)

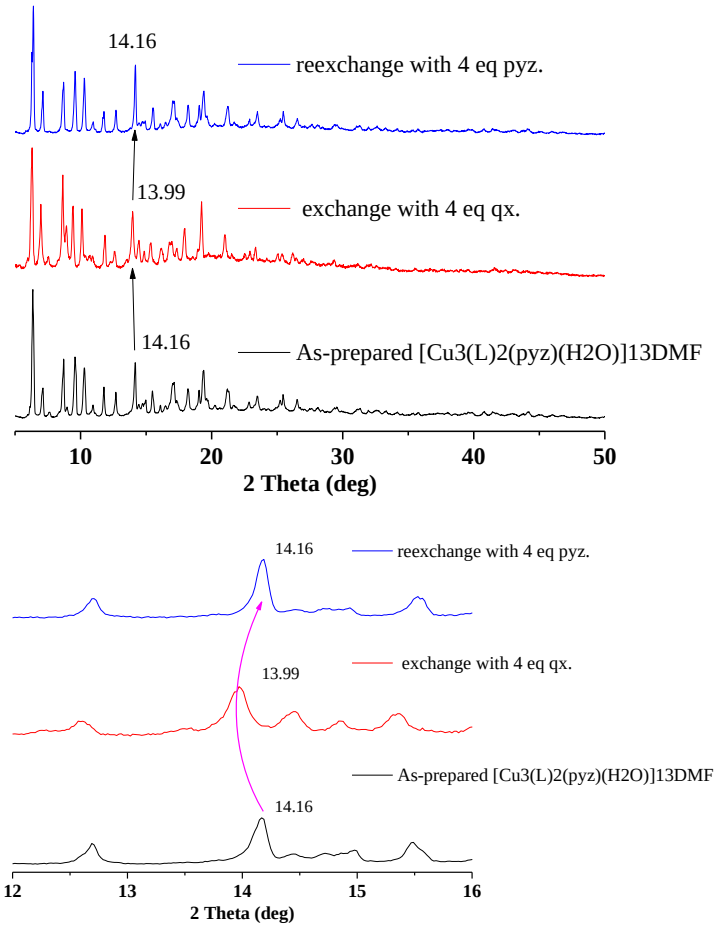

(b)

Fig. S7. (a) PXRD patterns for prepared **1-6** and simulated pattern from single crystal data **1**. (b) PXRD patterns for the ligand exchange.

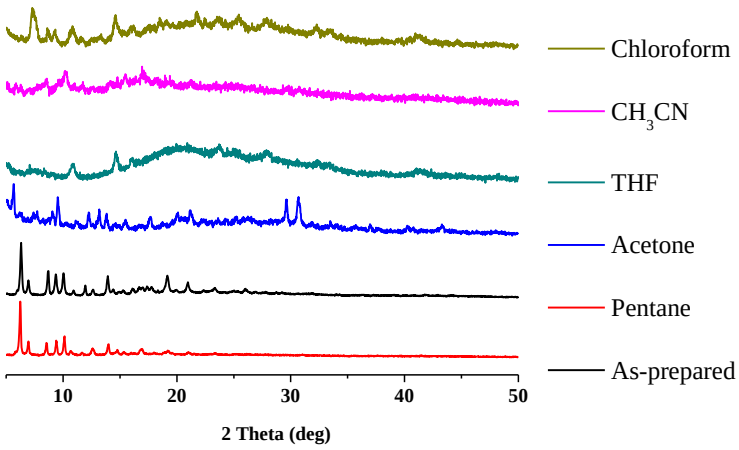

Fig. S8. PXRD patterns of **4** after immersing in different solvents.

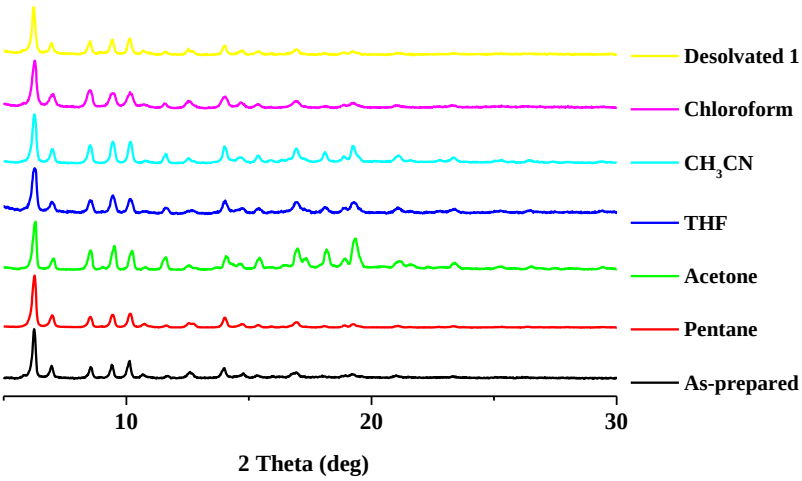

Fig. S9. PXRD patterns of **1** after immersing in different solvents and activation.

^{1}H-NMR spectral data

The obtained MOFs were digested in ($Na_2S/D_2O/DMSO\text{-}d_6$), this allowed for monitoring the hydrogen atoms from pyrazine derivatives in the MOFs. In all ^{1}H-NMR spectra, peak around δ = 8.18, 7.98, 7.85 and 7.68 correspond to the proton from L^{3-}. 7.93, 2.89 and 2.72 are from DMF. The other peaks are attributed to the proton from pyz or its derivatives.

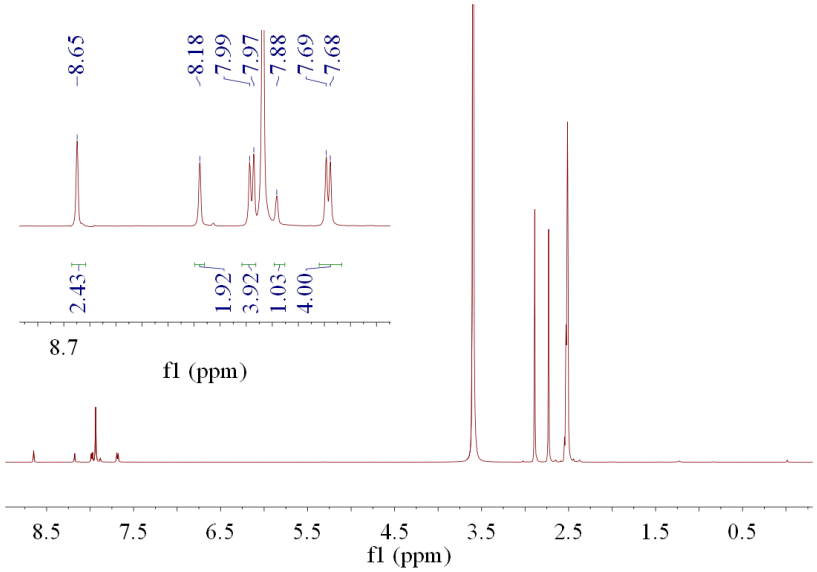

Fig. S10. ^{1}H-NMR spectrum of digested **1** (peak at δ = 8.65 corresponds to the protons from pyz).

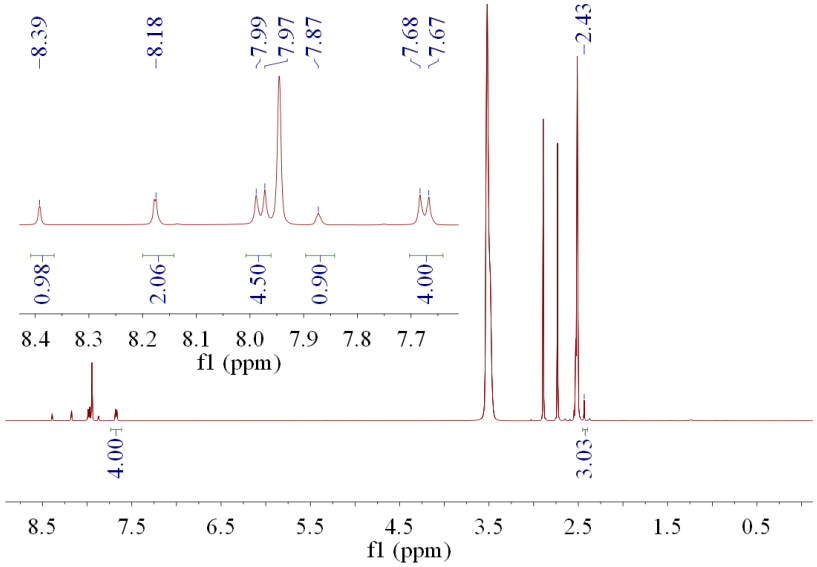

Fig. S11. ^{1}H-NMR spectrum of digested **2** (peaks at δ = 8.39 and 2.43 correspond to the protons from 2,5-Me_2pyz).

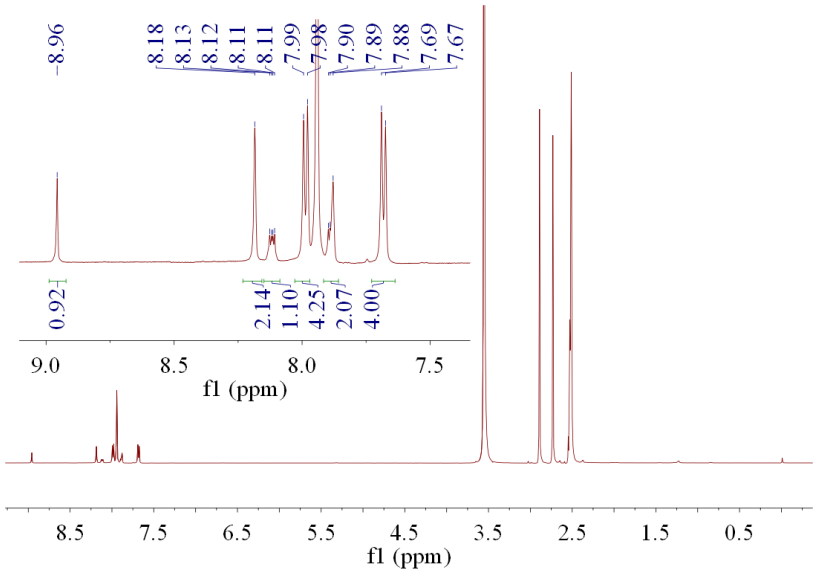

Fig. S12. ^{1}H-NMR spectrum of digested **3** (peaks at δ = 8.96, 8.11 and 7.88 correspond to the protons from qx).

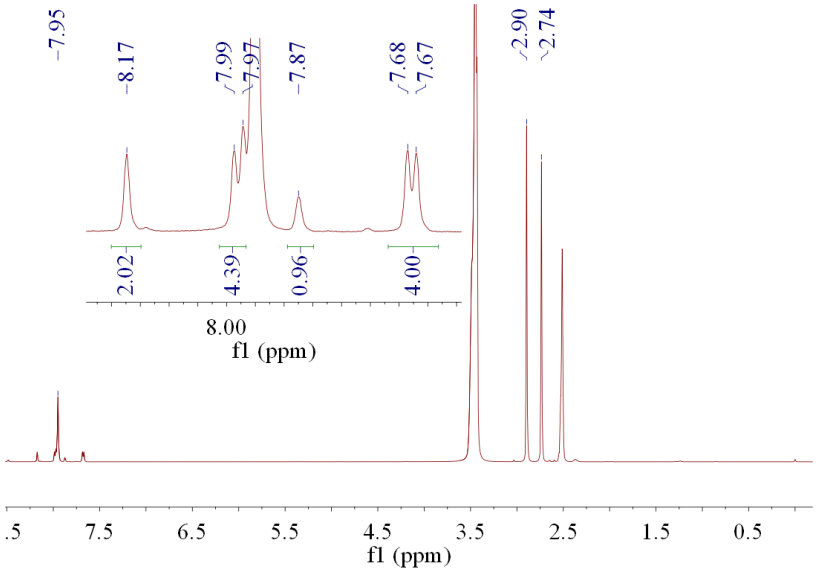

Fig. S13. ^{1}H-NMR spectrum of digested **4**.

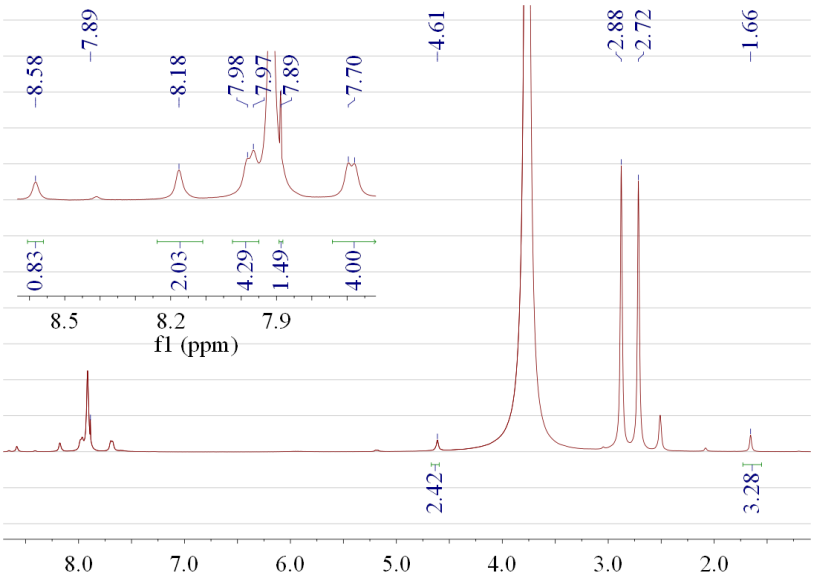

Fig. S14. ^{1}H-NMR spectrum of digested **5** (peaks at δ = 1.66, 4.61, 8.58 correspond to the protons from 2,5-$(C_3H_5O_2)_2$-pyz).

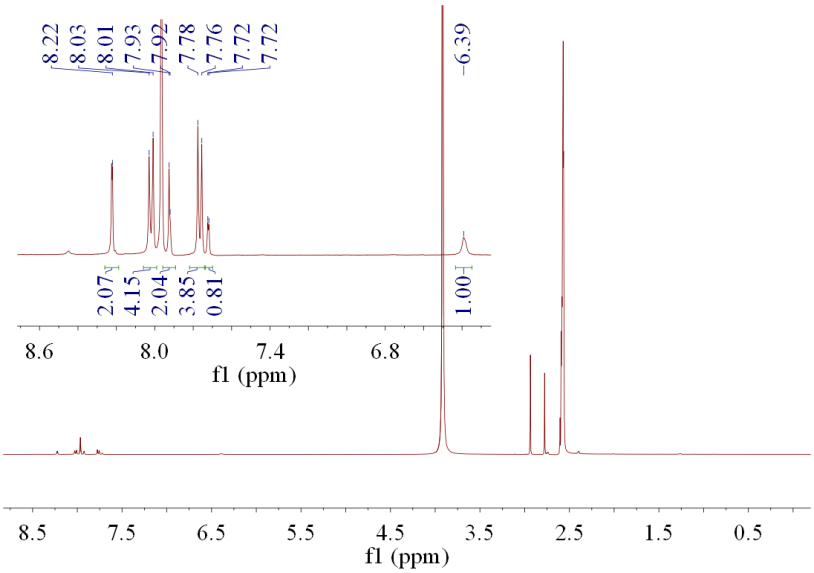

Fig. S15. ^{1}H-NMR spectrum of digested **6** (peaks at δ = 6.39, 7.72, 7.93 correspond to the protons from 2-NH_2-pyz).

Time-dependent X-ray diffraction analysis:

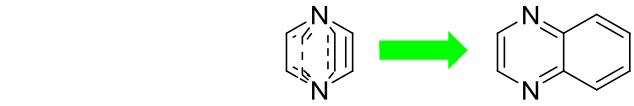

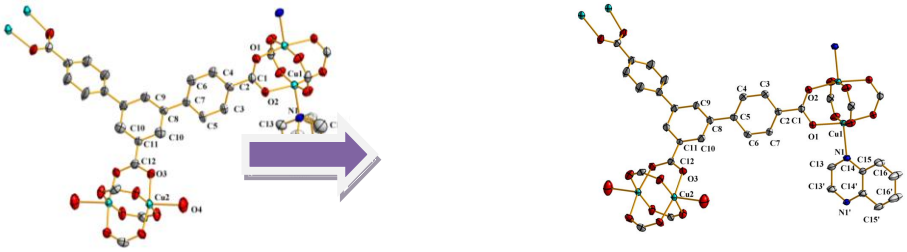

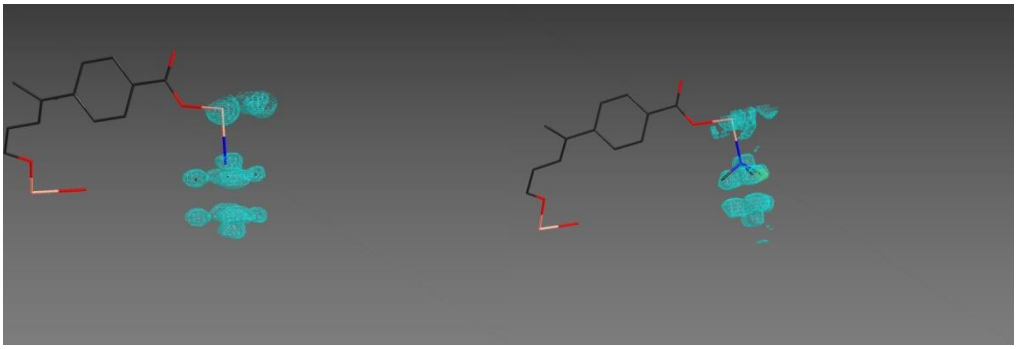

(a) (b)

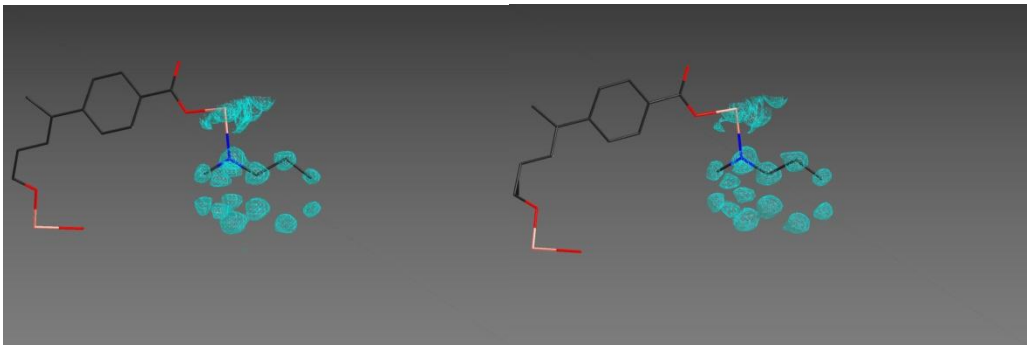

(c) (d)

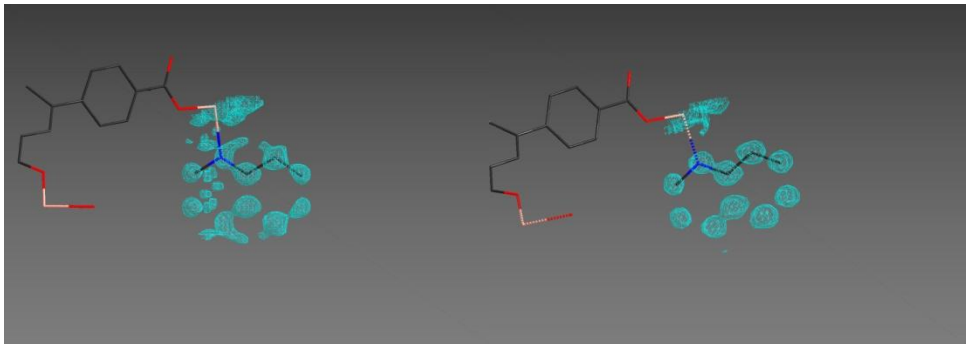

(e) (f)

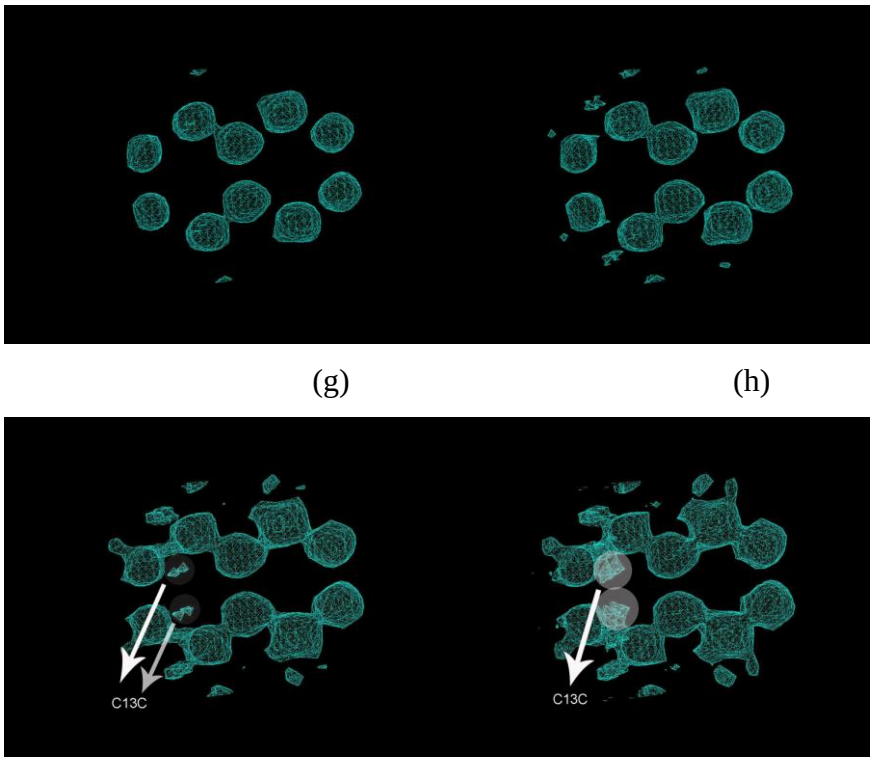

(g) (h)

(i) (j)

Fig. S16. Electron density maps (F_o) obtained by time-dependent X-ray diffraction in the reaction (a) before the injection, (b) after the injection 15 min - 3 h, (c) 5 h – 7 h, (d) 7 h – 9 h, (e) 19 h – 21 h, (f) 31h – 33 h. (g) - (j) Electron density maps contoured at different σ levels, namely 1.00 σ level for (g), 0.80 σ level for (h), 0.60 σ level for (i) and 0.50 σ level for (j).

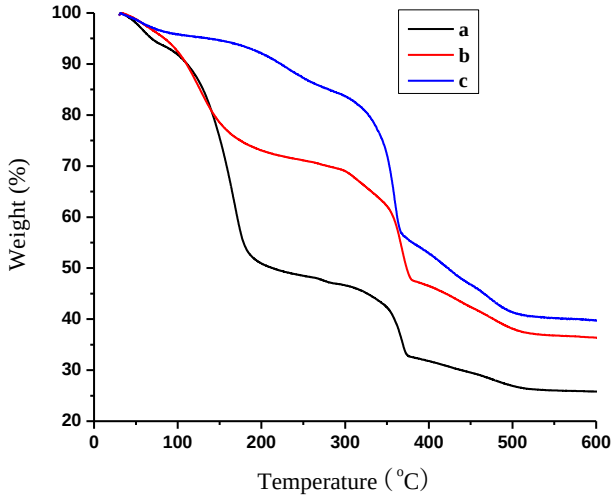

Fig. S17. TG curves of **1**: (a) the as-synthesized sample, (b) exchanged by acetone and (c) desolvated sample obtained by heating the acetone-exchanged sample at 423 K under vacuum for 4 h.

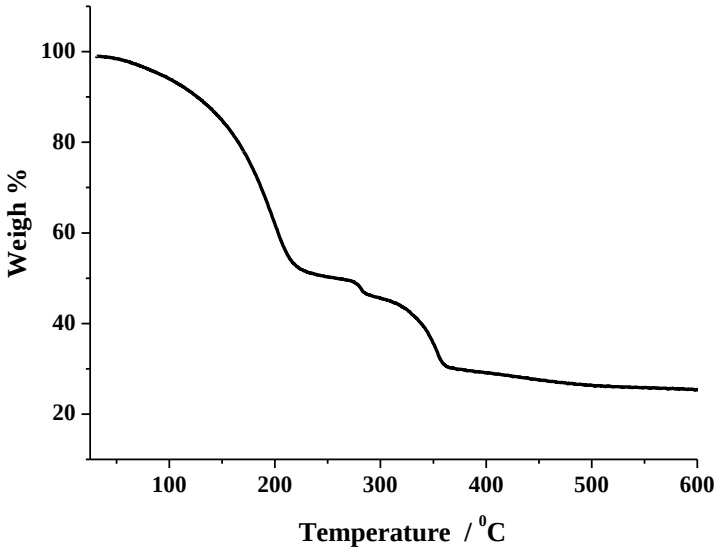

Fig. S18. TG curve of the as-synthesized **2**.

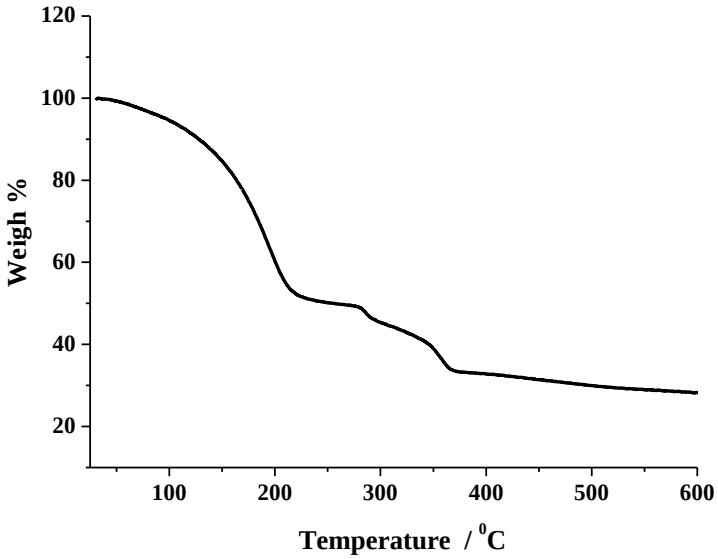

Fig. S19. TG curve of the as-synthesized **3**.

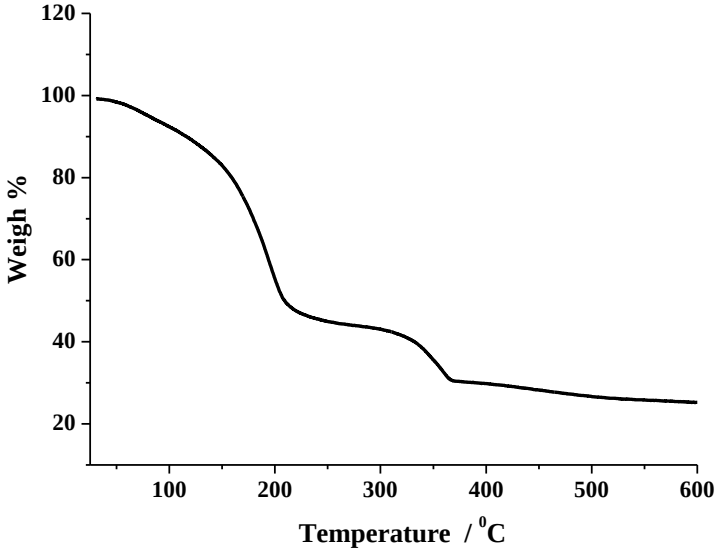

Fig. S20. TG curve of the as-synthesized **4**.

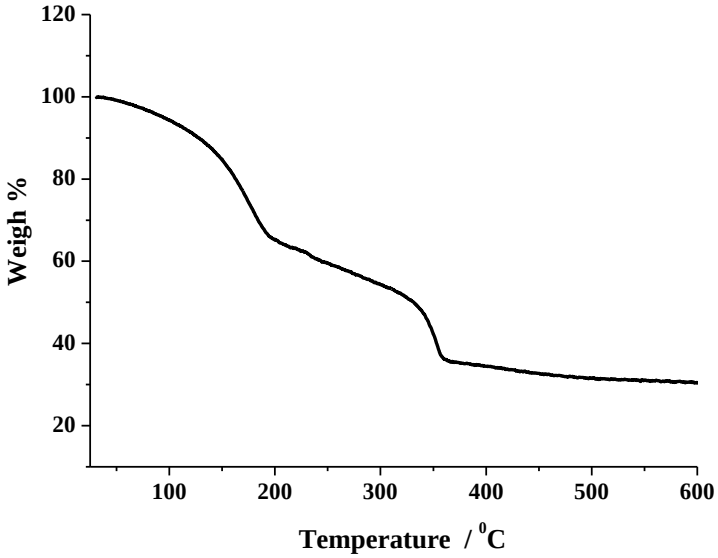

Fig. S21. TG curve of the as-synthesized **5**.

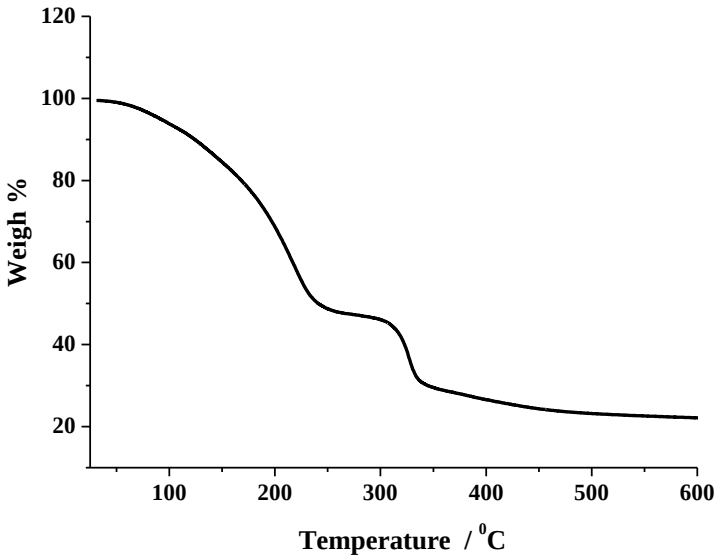

Fig. S22. TG curve of the as-synthesized **6**.

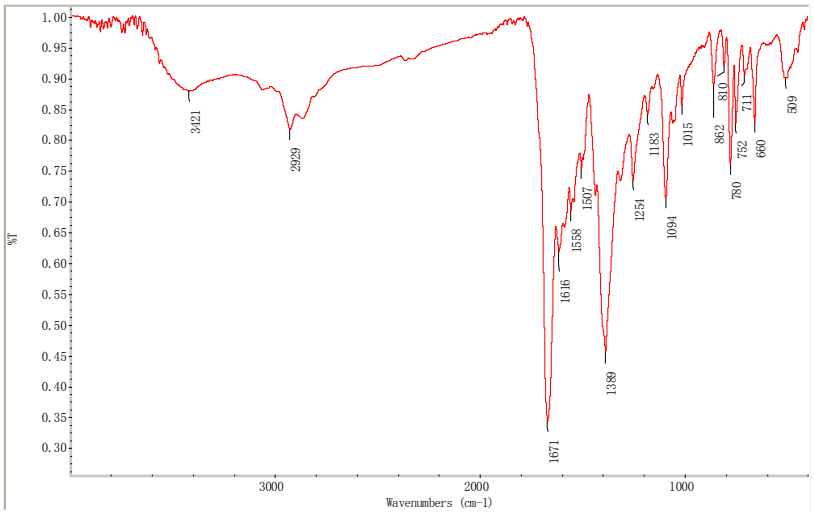

Fig. S23. FT-IR spectrum of the as-synthesized **1**.

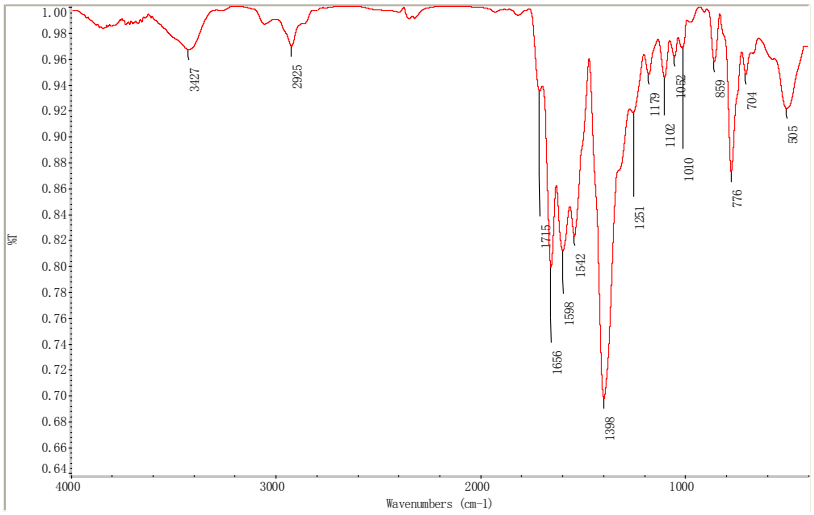

Fig. S24. FT-IR spectrum of the as-synthesized **2**.

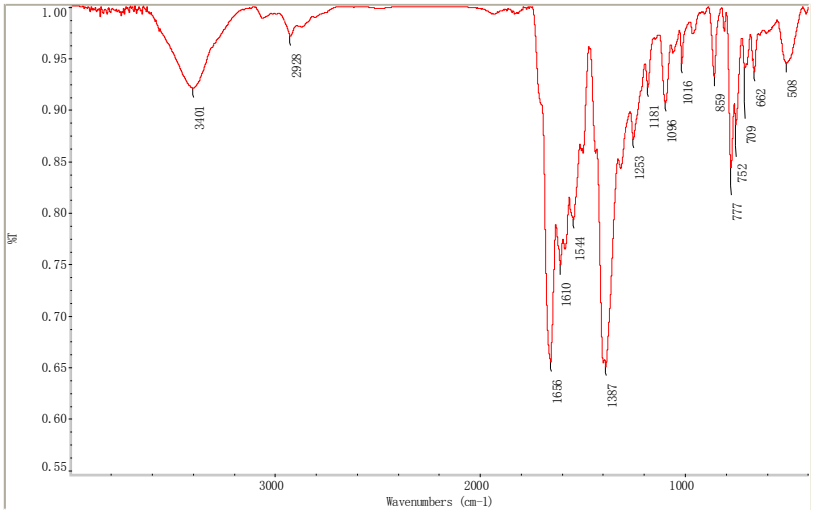

Fig. S25. FT-IR spectrum of the as-synthesized **3**.

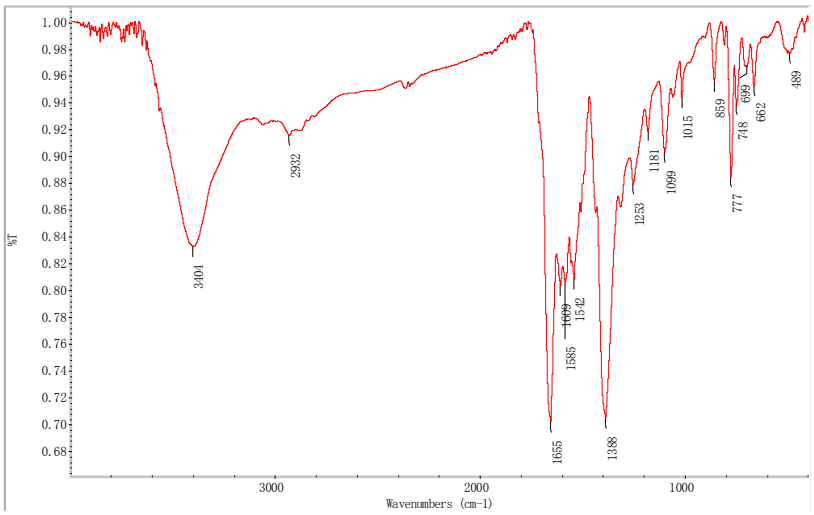

Fig. S26. FT-IR spectrum of the as-synthesized **4**.

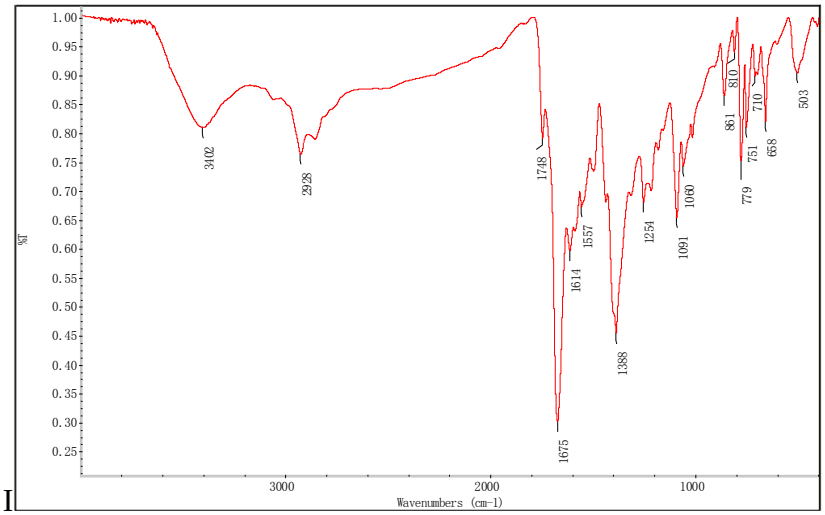

Fig. S27. FT-IR spectrum of the as-synthesized **5**.

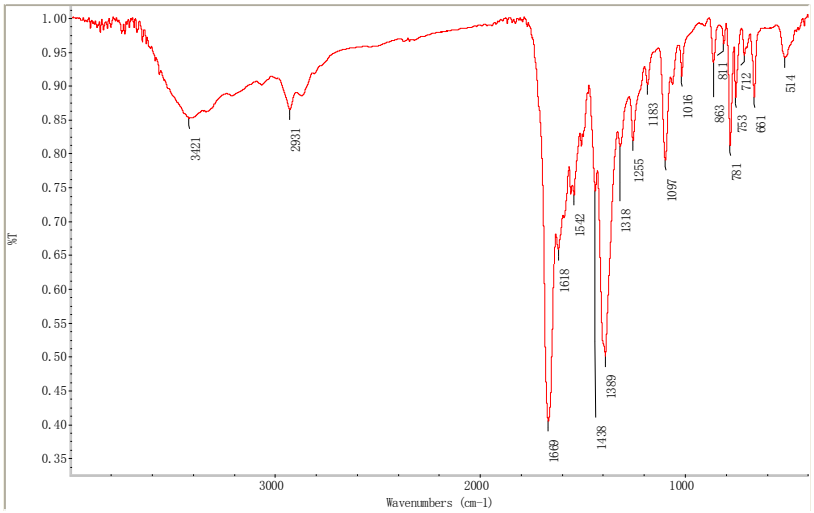

Fig. S28. FT-IR spectrum of the as-synthesized **6**.

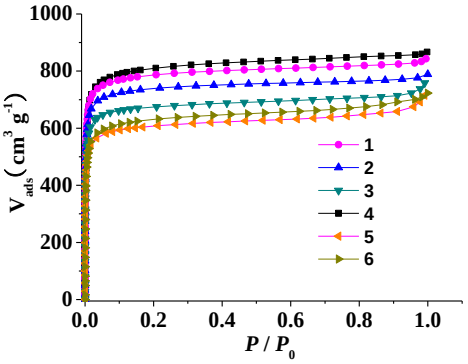

Fig. S29. N_2 adsorption isotherms of **1** - **6** at 77 K.

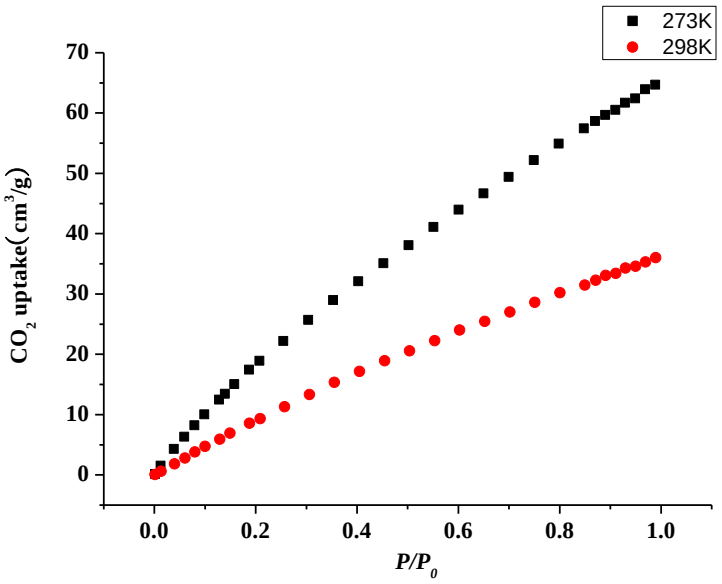

(a)

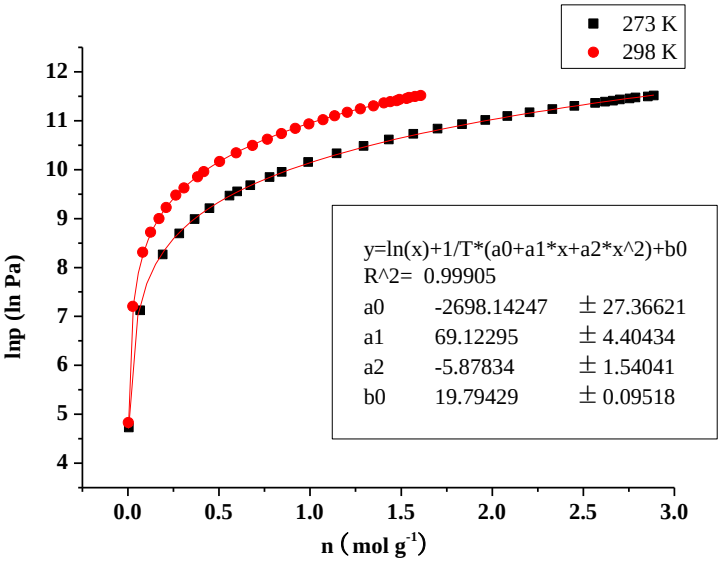

(b)

Fig. S30. CO_2 adsorption isotherms for **1** at 273 and 298 K. (b) CO_2 adsorption isotherms for **1** with fitting by virial method.

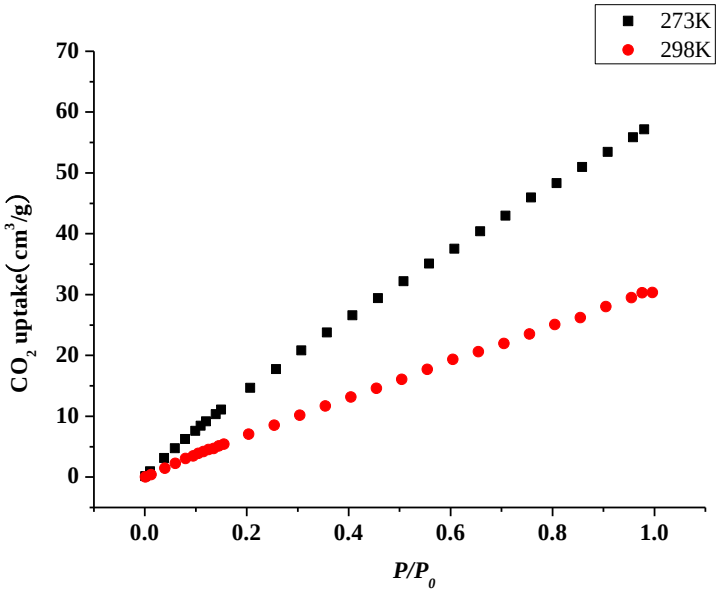

(a)

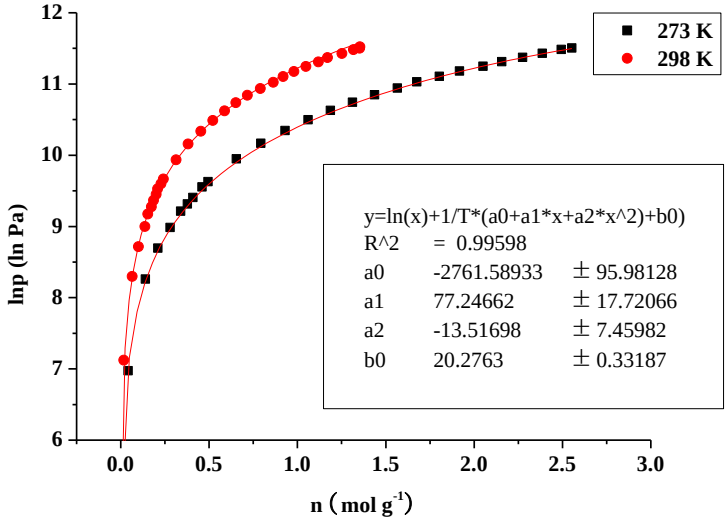

(b)

Fig. S31. (a) CO_2 adsorption isotherms for **2** at 273 and 298 K. (b) CO_2 adsorption isotherms for **2** with fitting by virial method.

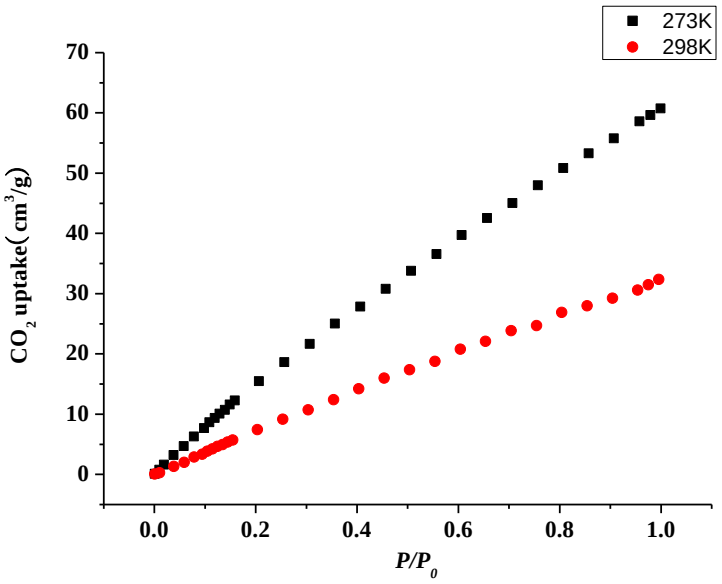

(a)

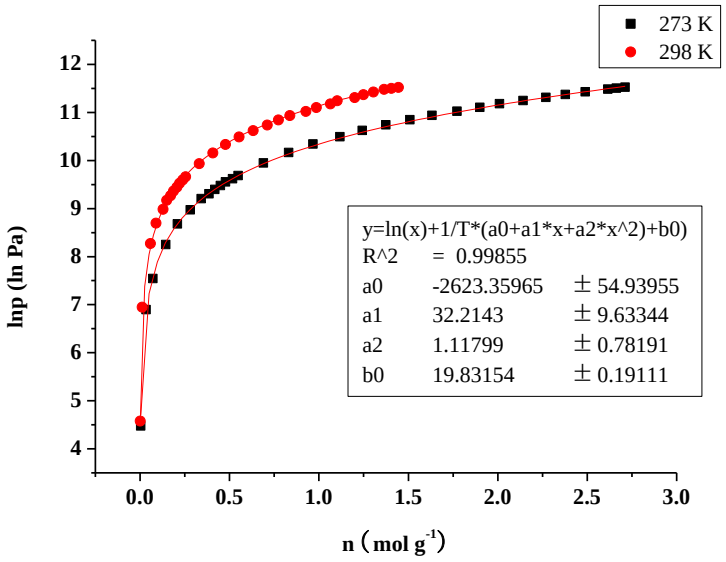

(b)

Fig. S32. (a) CO_2 adsorption isotherms for **3** at 273 and 298 K. (b) CO_2 adsorption isotherms for **3** with fitting by virial method.

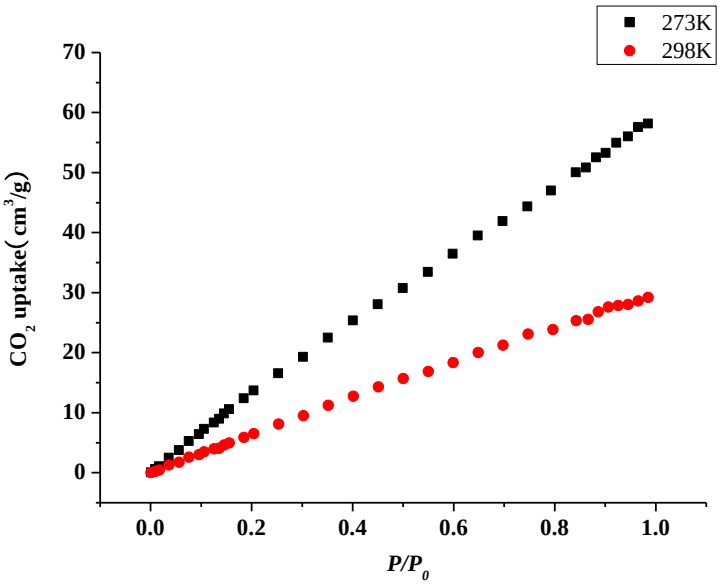

(a)

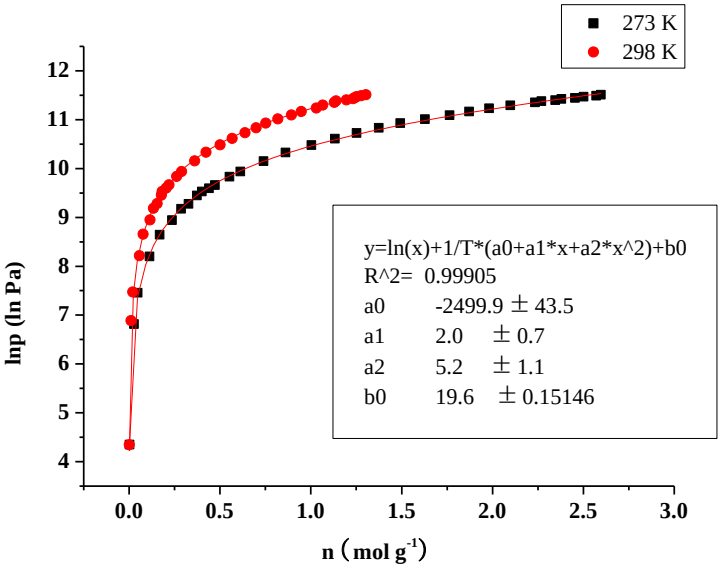

(b)

Fig. S33. (a) CO_2 adsorption isotherms for **4** at 273 and 298 K. (b) CO_2 adsorption isotherms for **4** with fitting by virial method.

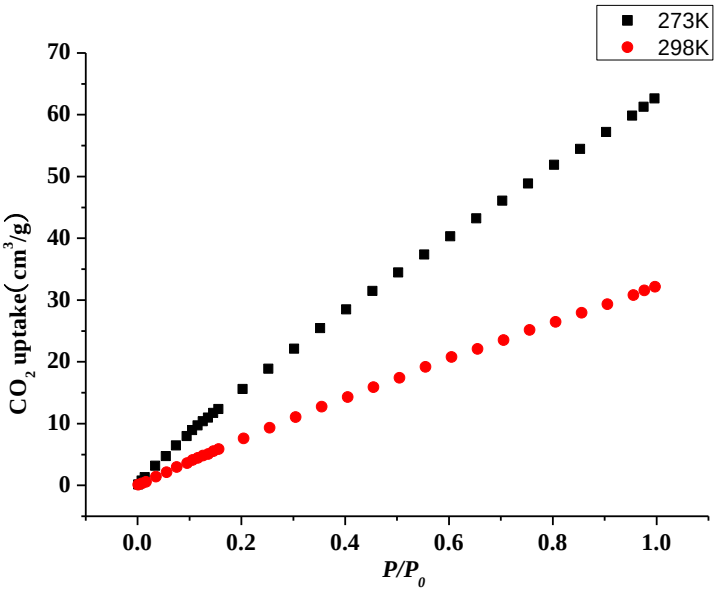

(a)

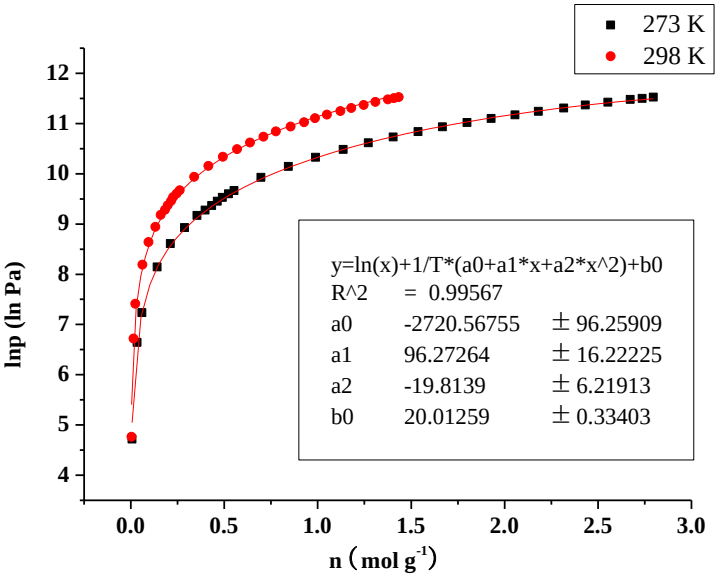

(b)

Fig. S34. (a) CO_2 adsorption isotherms for **5** at 273 and 298 K. (b) CO_2 adsorption isotherms for **5** with fitting by virial method.

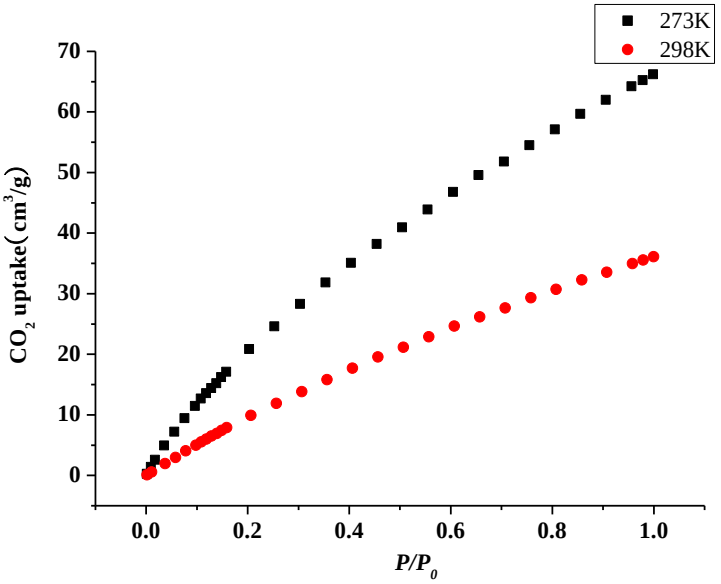

(a)

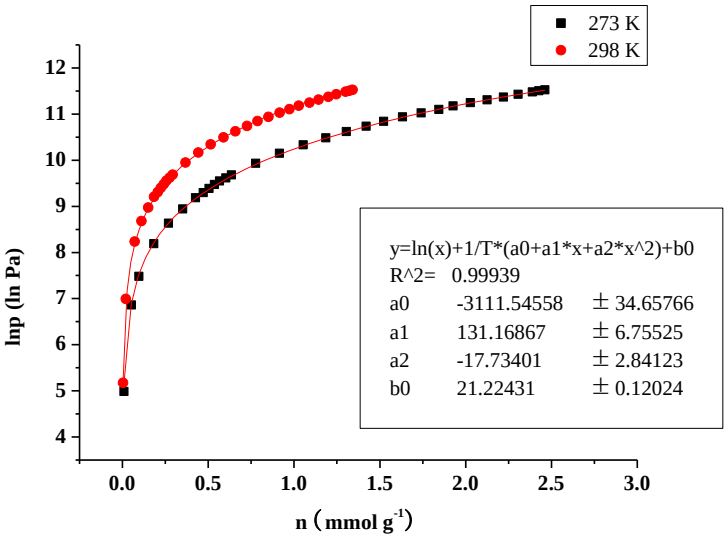

(b)

Fig. S35. (a) CO_2 adsorption isotherms for **6** at 273 and 298 K. (b) CO_2 adsorption isotherms for **6** with fitting by virial method.

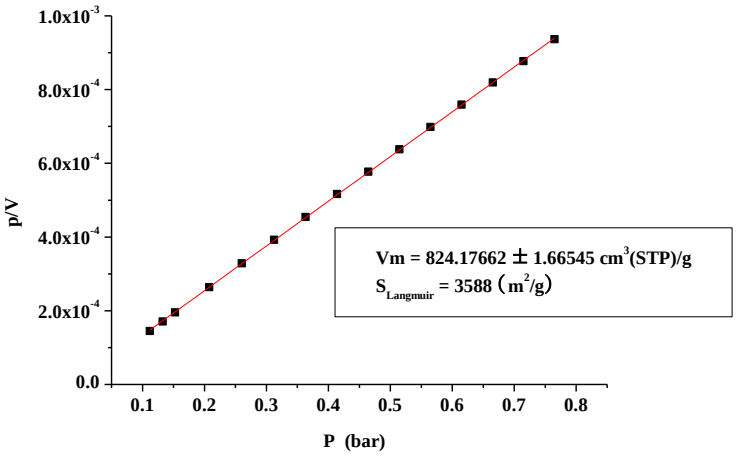

(a)

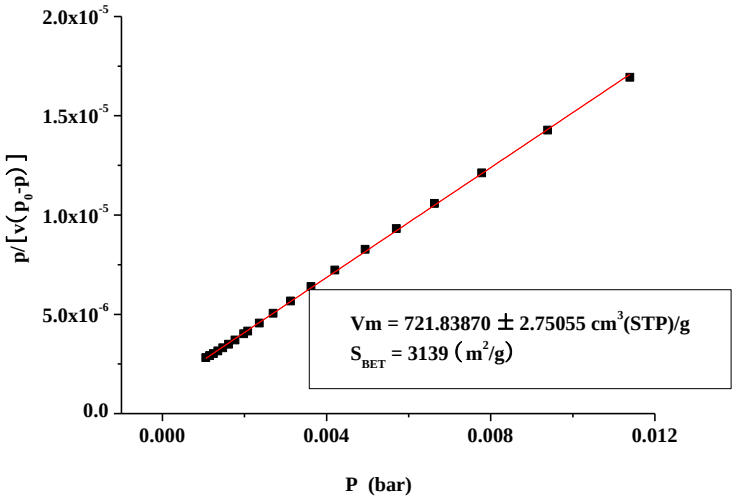

(b)

Fig. S36. The Langmuir (a) and BET (b) plots calculated from N_2 isotherm of **1**.

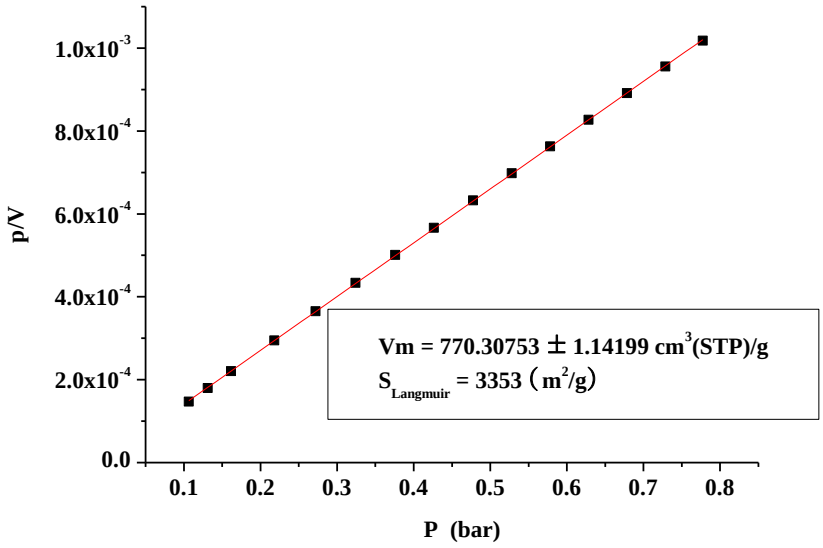

(a)

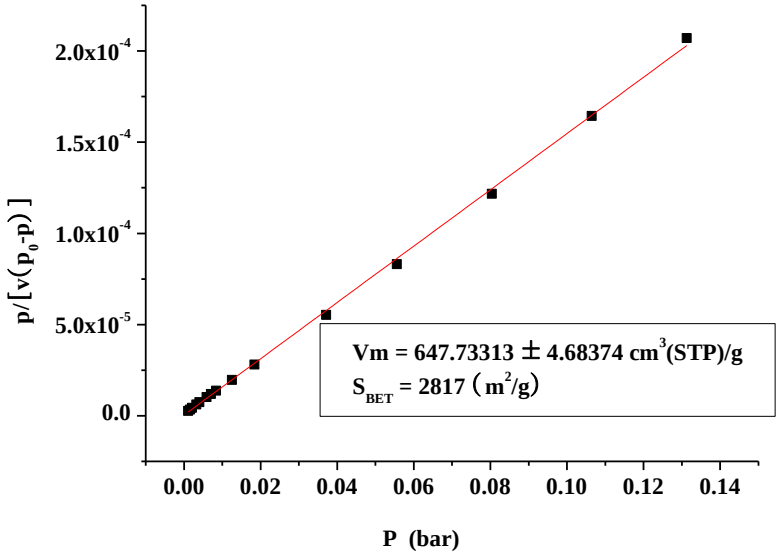

(b)

Fig. S37. The Langmuir (a) and BET (b) plots calculated from N_2 isotherm of **2**.

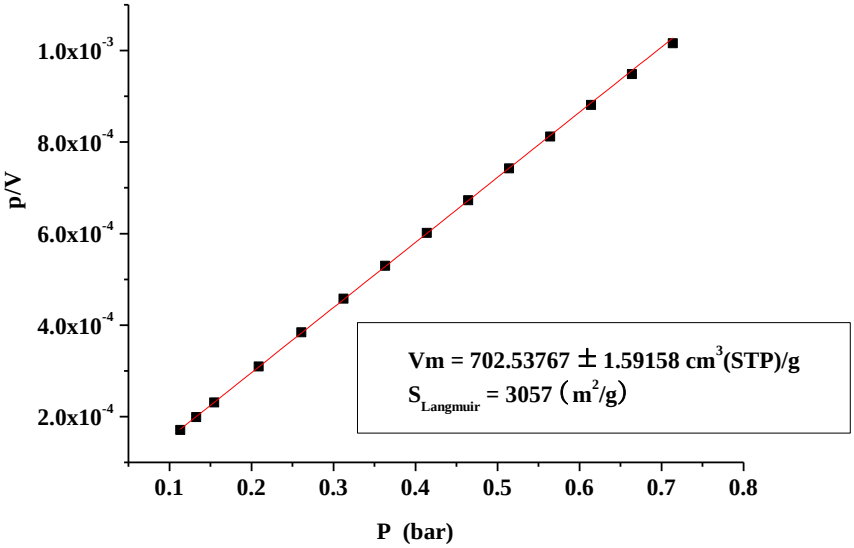

(a)

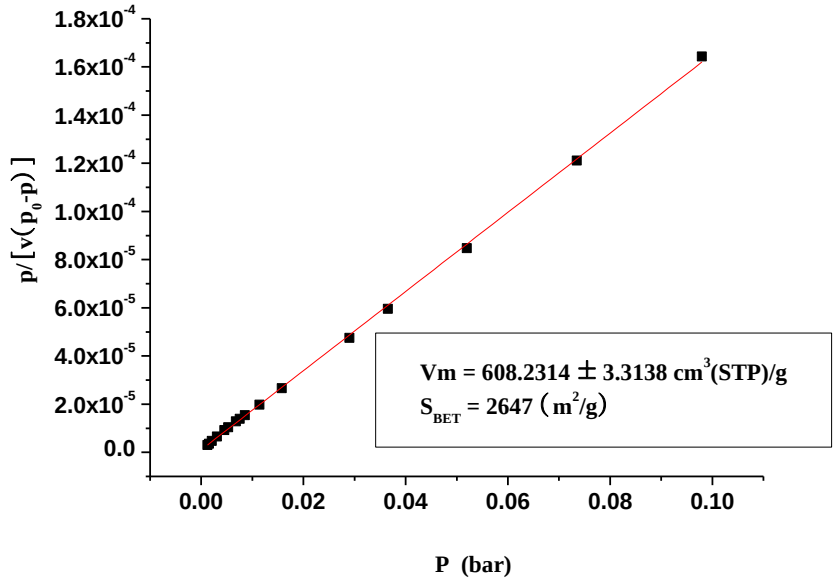

(b)

Fig. S38. The Langmuir (a) and BET (b) plots calculated from N_2 isotherm of **3**.

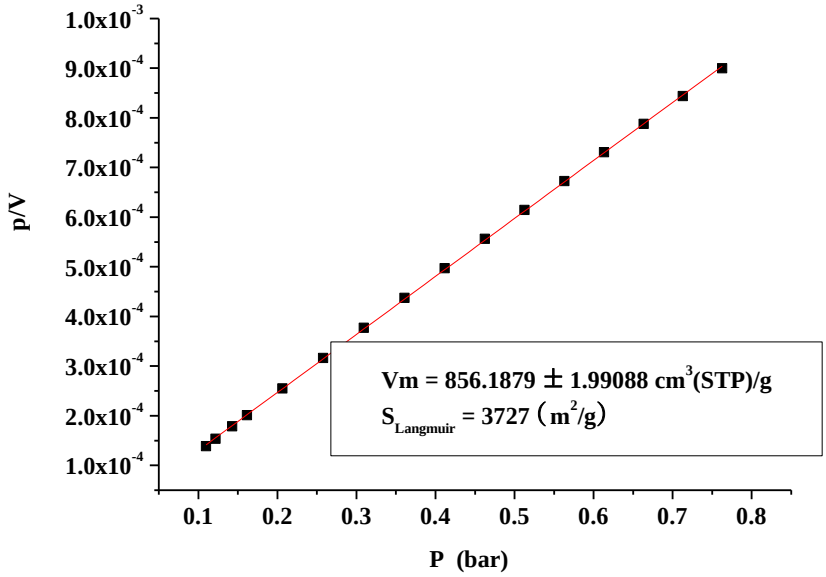

(a)

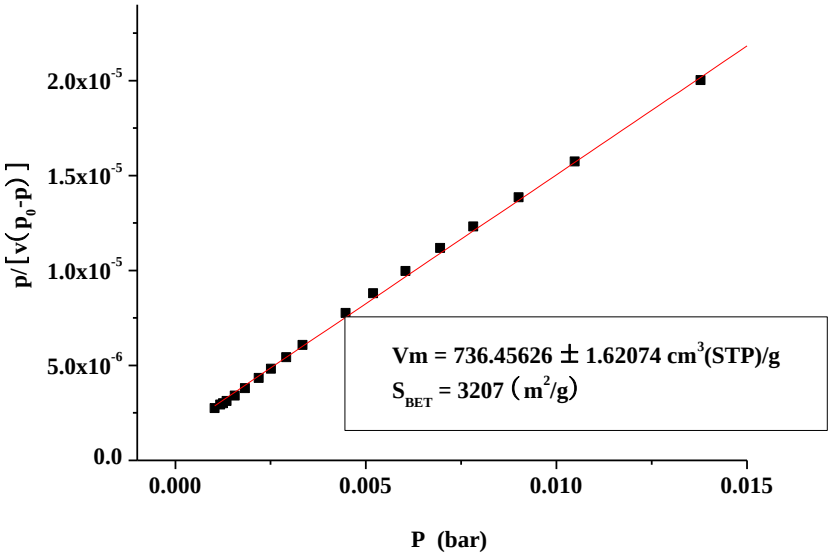

(b)

Fig. S39. The Langmuir (a) and BET (b) plots calculated from N_2 isotherm of **4**.

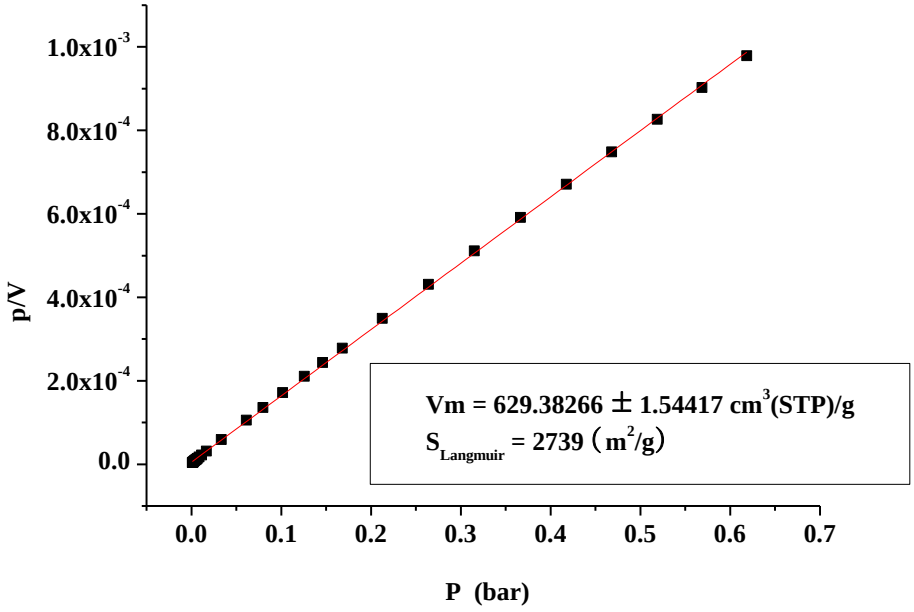

(a)

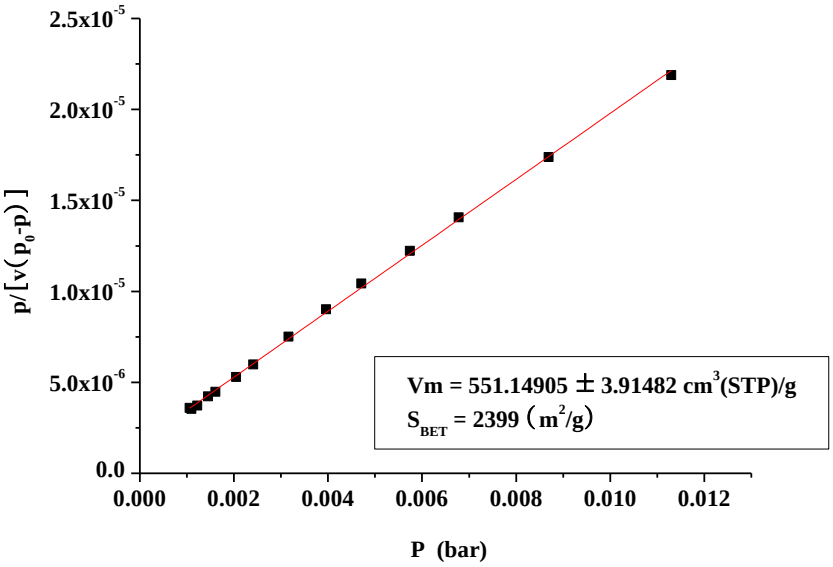

(b)

Fig. S40. The Langmuir (a) and BET (b) plots calculated from N_2 isotherm of **5**.

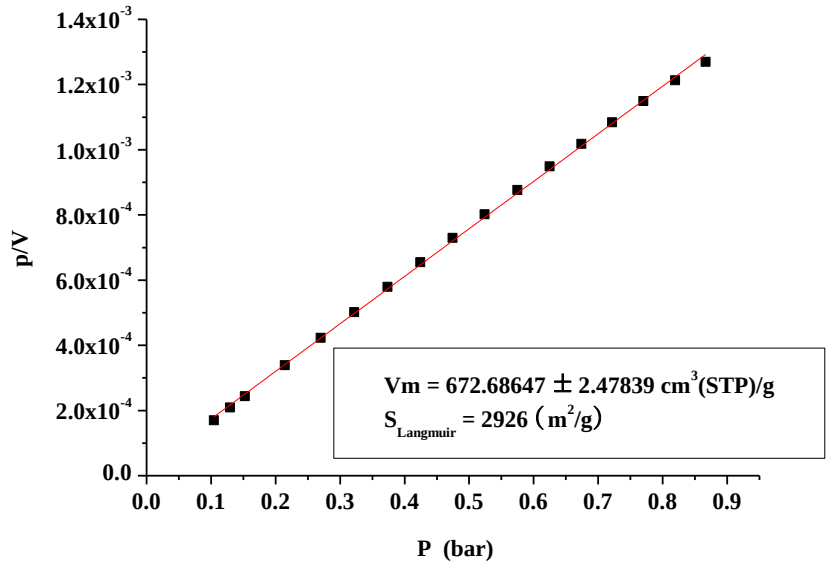

(a)

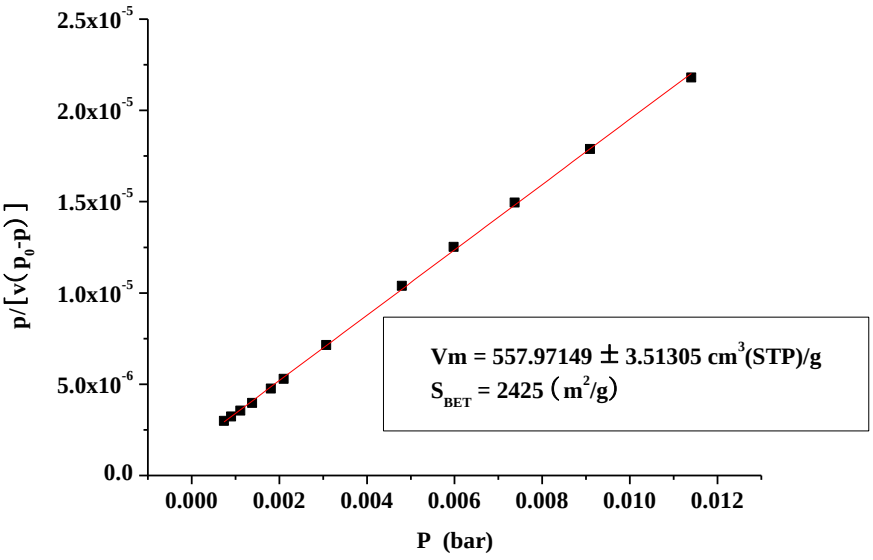

(b)

Fig. S41. The Langmuir (a) and BET (b) plots calculated from N_2 isotherm of **6**.

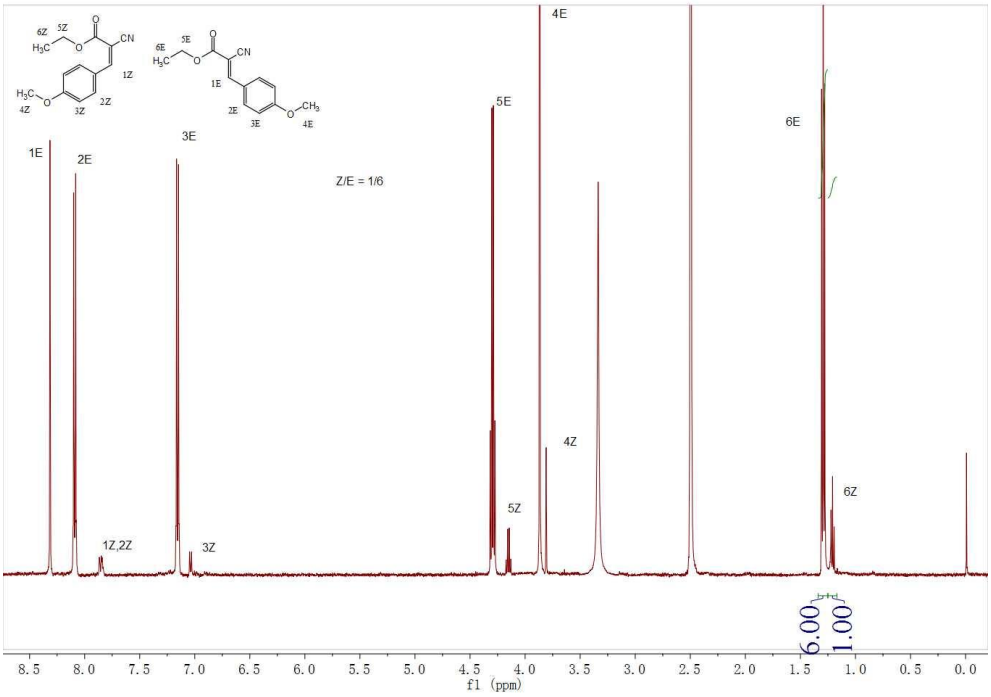

(a)

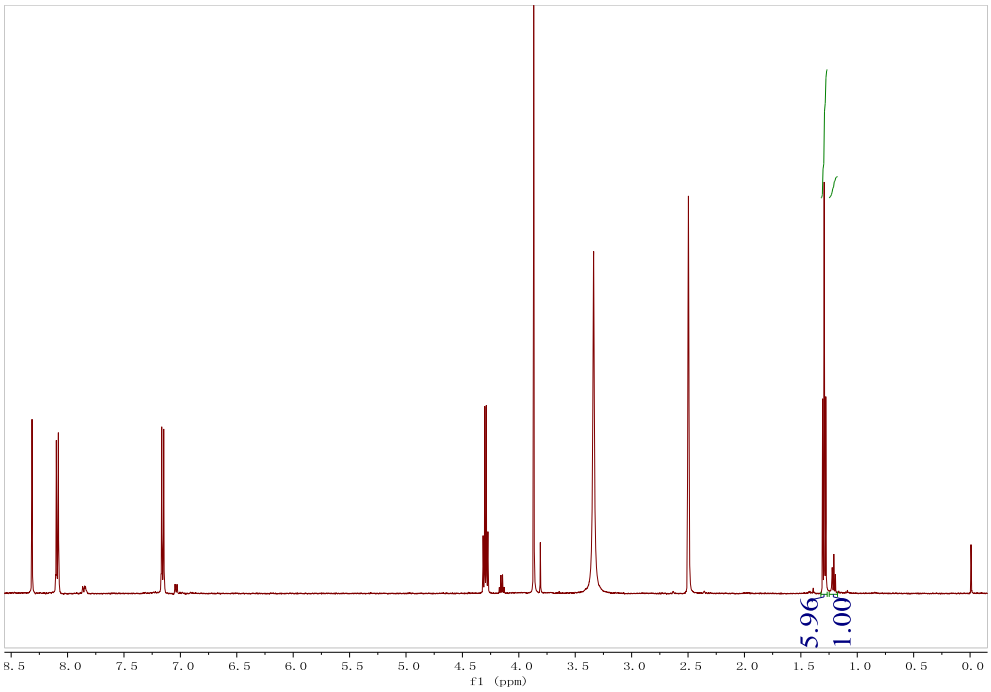

(b)

Fig. S42. ^{1}H NMR spectra of (*E*)/(Z)-ethyl 2-cyano-3-(4-methoxyphenyl)acrylate in DMSO-d_6 at room temperature. (a) Before the reaction with MOF: *E* : *Z* = 6 : 1. (b) After the reaction with MOF under the conditions of the condensation reaction for 24 h: *E* : *Z* = 6 : 1.

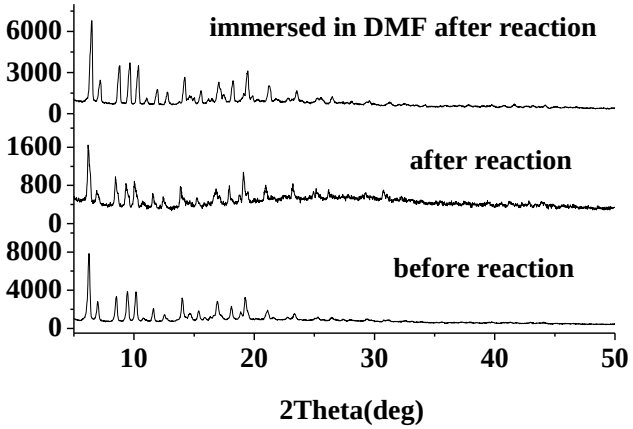

Fig. S43. PXRD patterns for MOF **6** before and after the reaction and re-immersed in DMF after reaction.

Table S1. Crystal data and structure refinements for **1 - 6**

	1	**2**	**3**	**4**	**5**	**6**
Empirical formula	$C_{85}H_{119}Cu_3N_{15}O_{26}$	$C_{168}H_{232}Cu_6N_{28}O_{50}$	$C_{86}H_{114}Cu_3N_{14}O_{25}$	$C_{78}H_{112}Cu_3N_{12}O_{27}$	$C_{152}H_{184}Cu_6N_{20}O_{50}$	$C_{164}H_{226}Cu_6N_{30}O_{50}$
Formula weight	1957.56	3825.04	1934.53	1840.41	3472.42	3798.97
Crystal system	Tetragonal	Tetragonal	Tetragonal	Tetragonal	Tetragonal	Tetragonal
Space group	$I4_1/amd$	$I4_1/amd$	$I4_1/amd$	$I4_1/amd$	$I4_1/amd$	$I4_1/amd$
a (Å)	19.387(4)	19.511(2)	19.730(4)	20.009(1)	19.627(2)	19.525(5)
b (Å)	19.387(4)	19.511(2)	19.730(4)	20.009(1)	19.627(2)	19.525(5)
c (Å)	60.831(13)	60.340(7)	60.06(1)	59.029(7)	60.175(6)	60.38(2)
T (K)	293(2)	293(2)	293(2)	293(2)	293(2)	293(2)
V (Å^3)	22864(11)	22970(5)	23380(10)	23633(4)	23181(5)	23018(14)
Z	8	4	8	8	4	4
ρ_{calcd} (g cm^{-3})	1.137	1.106	1.099	1.035	0.995	1.096
μ (mm^{-1})	0.620	0.615	0.605	0.596	0.603	0.614
F(000)	8232	8040	8120	7736	7240	7976
Data collected	31263	89079	78053	79082	66775	59272
Independent data	5792	5810	7116	7172	5808	5434
Goodness-of-fit	1.029	1.031	1.020	1.106	1.120	1.006
R_1[a] ($I > 2\sigma(I)$)	0.0599	0.0737	0.0417	0.0643	0.0738	0.0561
wR_2[b] ($I > 2\sigma(I)$)	0.1217	0.2229	0.1334	0.2132	0.1863	0.1542

[a] $R_1 = \Sigma||F_o| - |F_c||/\Sigma|F_o|$. [b] $wR_2 = |\Sigma w(|F_o|^2 - |F_c|^2)|/\Sigma|w(F_o)^2|^{1/2}$, where $w = 1/[\sigma^2(F_o^2) + (aP)^2 + bP]$. $P = (F_o^2 + 2F_c^2)/3$.

Table S2. Selected bond lengths (Å) and angles (°) for **1** – **6** [a]

1			
Cu(1)-O(1)#1	1.947(3)	Cu(2)-O(3)#4	1.932(3)
Cu(1)-O(2)#3	1.976(3)	Cu(2)-O(4)	2.196(7)
Cu(1)-N(1)	2.202(5)	O(1)#1-Cu(1)-O(1)#2	88.7(2)
O(3)#4-Cu(2)-O(3)	168.53(17)	O(1)#1-Cu(1)-O(2)	167.58(13)
O(3)-Cu(2)-O(3)#5	89.5(2)	O(1)#2-Cu(1)-O(2)	89.97(13)
O(3)-Cu(2)-O(3)#6	89.3(2)	O(2)-Cu(1)-O(2)#3	88.7(2)
O(3)#4-Cu(2)-O(4)	95.74(9)	O(1)#1-Cu(1)-N(1)	97.28(15)
O(2)-Cu(1)-N(1)	95.14(15)		
2			
Cu(1)-O(1)#1	1.948(4)	Cu(2)-O(3)	1.940(4)
Cu(1)-O(2)	1.954(3)	Cu(2)-O(4)	2.137(8)
Cu(1)-N(1)	2.227(5)	O(1)#1-Cu(1)-O(1)#2	88.6(2)
O(3)-Cu(2)-O(4)	96.06(10)	O(1)#1-Cu(1)-O(2)	168.50(15)
O(3)-Cu(2)-O(3)#5	89.6(2)	O(1)#2-Cu(1)-O(2)	90.37(16)
O(3)-Cu(2)-O(3)#6	89.1(2)	O(2)-Cu(1)-O(2)#3	88.3(2)
O(2)-Cu(1)-N(1)	95.16(15)	O(1)#1-Cu(1)-N(1)	96.33(15)
3			
Cu(1)-O(2)#1	1.957(2)	Cu(2)-O(3)	1.961(2)
Cu(1)-O(1)	1.969(2)	Cu(2)-O(4)	2.205(5)
Cu(1)-N(1)	2.225(3)	O(2)#1-Cu(1)-O(2)#2	88.20(14)
O(1)-Cu(1)-N(1)	94.16(9)	O(2)#1-Cu(1)-O(1)	168.13(9)
O(3)#4-Cu(2)-O(3)#5	88.95(14)	O(2)#2-Cu(1)-O(1)	91.04(10)
O(3)#4-Cu(2)-O(3)#6	89.72(14)	O(1)-Cu(1)-O(1)#3	87.28(14)
O(3)#4-Cu(2)-O(4)	96.18(6)	O(2)#1-Cu(1)-N(1)	97.68(10)
4			
Cu(1)-O(1)	1.953(3)	Cu(2)-O(3)	1.957(3)
Cu(1)-O(2)#2	1.949(3)	Cu(2)-O(4)	2.123(8)
Cu(1)-O(5)	2.093(5)	O(1)#1-Cu(1)-O(1)	88.2(2)
O(2)#2-Cu(1)-O(5)	94.08(15)	O(1)#1-Cu(1)-O(2)#2	90.75(14)
O(3)#4-Cu(2)-O(3)	168.27(17)	O(1)-Cu(1)-O(2)#2	169.67(15)
O(3)#4-Cu(2)-O(3)#5	89.40(18)	O(1)-Cu(1)-O(5)	96.25(16)

O(3)-Cu(2)-O(3)#5	89.40(19)	O(2)#2-Cu(1)-O(2)#3	88.4(2)
O(3)-Cu(2)-O(4)	95.87(8)		
5			
Cu(1)-O(1)#1	1.948(3)	Cu(2)-O(3)	2.168(7)
Cu(1)-O(2)	1.964(3)	Cu(2)-O(4)	1.967(3)
Cu(1)-N(1)	2.202(7)	O(1)#1-Cu(1)-O(1)#2	88.4(2)
O(2)-Cu(1)-N(1)	94.62(18)	O(1)#1-Cu(1)-O(2)	90.41(15)
O(4)-Cu(2)-O(4)#5	89.6(2)	O(1)#2-Cu(1)-O(2)	168.48(15)
O(4)-Cu(2)-O(4)#4	167.96(18)	O(1)#1-Cu(1)-N(1)	96.90(17)
O(4)#4-Cu(2)-O(4)#5	89.1(2)	O(2)-Cu(1)-O(2)#3	88.4(2)
O(3)-Cu(2)-O(4)	96.02(9)		
6			
Cu(1)-O(1)#1	1.953(3)	Cu(2)-O(3)	1.952(3)
Cu(1)-O(2)	1.963(3)	Cu(2)-O(4)	2.185(6)
Cu(1)-N(1)	2.181(5)	O(1)#1-Cu(1)-O(1)#2	87.39(17)
O(2)-Cu(1)-N(1)	94.91(12)	O(1)#1-Cu(1)-O(2)	167.60(12)
O(3)#4-Cu(2)-O(3)	168.59(15)	O(1)#2-Cu(1)-O(2)	90.87(12)
O(3)#4-Cu(2)-O(3)#5	89.74(17)	O(1)#2-Cu(1)-O(2)#3	167.60(12)
O(3)-Cu(2)-O(3)#5	89.13(17)	O(2)-Cu(1)-O(2)#3	88.20(17)
O(3)-Cu(2)-O(4)	95.70(8)	O(1)#1-Cu(1)-N(1)	97.49(12)

[a]Symmetry transformation used to generate equivalent atoms: **1**. #1, -x,-y,-z; #2, x,-y,-z; #3, -x,y,z; #4, -x+1,-y+1/2,z; #5, x,-y+1/2,z; #6, -x+1,y,z; #7, -y+3/4,-x+3/4,-z+1/4; **2**. #1, -x+1/2,y+0,-z+3/2; #2, -x+1/2,-y+3/2,-z+3/2; #3, x,-y+3/2,z; #4, -x+1,-y+5/2,z; #5, -x+1,y,z; #6, x,-y+5/2,z; **3**. #1, -x+1,-y+2,-z+1; #2, x,-y+2,-z+1; #3, -x+1,y,z; #4, -x+2,y,z #5, x,-y+3/2,z #6, -x+2,-y+3/2,z; **4**. #1, -x+2,y,z; #2, -x+2,-y+2,-z+2; #3, x,-y+2,-z+2; #4, -x+1,-y+3/2,z; #5, x,-y+3/2,z; #6, -x+1,y,z; **5**. #1, -x+1/2,y,-z+1/2; #2, -x+1/2,-y+3/2,-z+1/2; #3, x,-y+3/2,z; #4, -x,-y+1/2,z; #5, x,-y+1/2,z; **6**. #1, -x+3/2,-y+3/2,-z+3/2; #2, -x+3/2,y+0,-z+3/2; #3, x,-y+3/2,z; #4, -x+1,-y+1/2,z; #5, x,-y+1/2,z; #6, -x+1,y,z.

Table S3. Unit cell, BET and Langmuir surface areas, pore volumes, porosities and Q_{st}^{o} for the isoreticular MOFs

MOFs	Unit cell (a = b, c) [Å]	Surface area [m^2/g] BET / Langmuir	Volume (void/cell)	Porosity (%)	Q_{st}^{o} (kJ/mol)
1	19.387, 60.83	3588/3139	16323.8/22864	71.37	22.40
2	19.511, 60.341	3353/2817	15348.3/22971	66.81	22.92
3	19.730, 60.062	3057/2647	16719.6/23381	71.50	21.79
4	20.009, 59.027	3727/3207	17708.7/23633	74.93	20.77
5	19.627, 60.175	2739/2399	13190.0/23181	56.90	22.57
6	19.525, 60.38	2926/2425	15892.7/23018	69.04	25.82
1-DABCO	19.156, 61.292	3154/2703	16229.1/22491	71.40	19.45

Table S4. Knoevenagel condensation of different benzaldehyde with ethyl cyanoacetate[a]

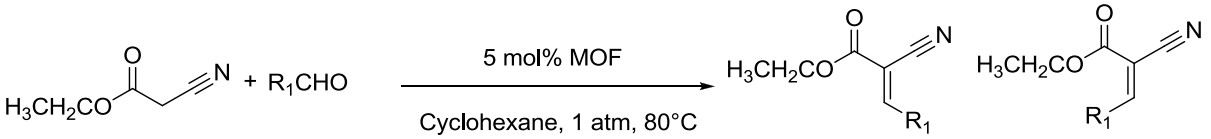

entry[a]		yield(%)[b]	*E* / *Z*
1	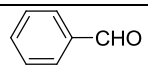	98 / 24	99 / 1
2	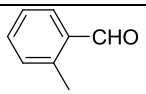	81 / 3	98 / 2
3	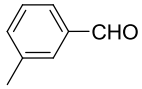	87 / 2	98 / 2
4	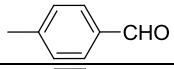	98 / 18	99 / 1
5	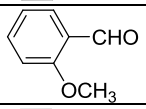	85 / 20	98 / 2
6	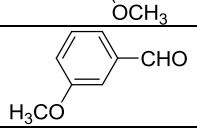	91 / 19	99 / 1
7	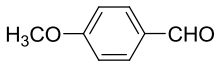	96 / 21	99 / 1
8	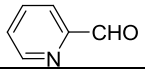	91 / 2	99 / 1
9	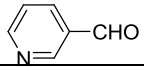	94 / 7	98 / 2
10	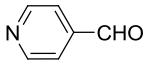	92 / 4	97 / 3

[a] 2 mmol benzaldehyde, 2 mmol ethyl cyanoacetate and 0.1 mmol the dried catalyst in 5 ml of cyclohexane at 353 K for 12 h.

[b] The yield with the MOF 6 as catalyst/ The yield without catalyst.

[c] *E/Z* = *E* isomers of corresponding Knoevenagel condensation products/*Z* isomers of corresponding Knoevenagel condensation products, which was determined by the intergration of vinylic proton in the complexes by ^{1}H-NMR.

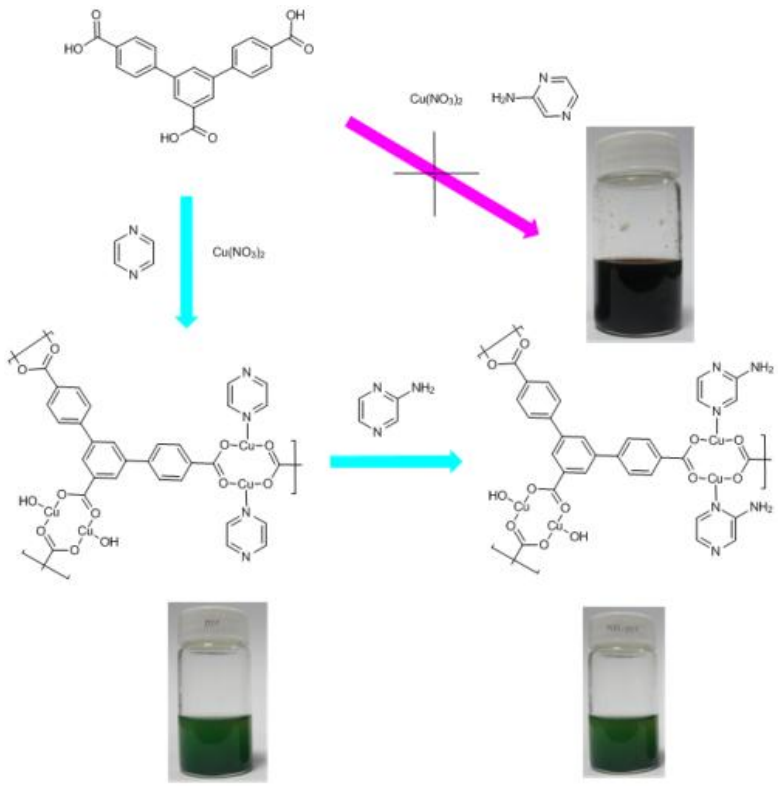

Scheme S1. Schematic illustration of conversion of **1** to **6** $[Cu_3(L)_2(pyz)(H_2O)]\cdot 13DMF$ (**1**), followed by ligand exchange to generate $[Cu_3(L)_2(2\text{-}NH2\text{-}pyz)(H2O)]\cdot 12DMF$ (**6**)

Experimental

Materials. The known compounds H_3L and 2,5-$(C_3H_5O_2)_2$-pyz were prepared by reported method.[1,2] Other chemicals and reagents are commercially available and were used without further purification.

Measurements. Elemental analyses for C, H, and N were performed on a Perkin-Elmer 240C Elemental Analyzer. Thermogravimetric analyses (TGA) were performed on a simultaneous SDT 2960 thermal analyzer under nitrogen with a heating rate of 10 K min^{-1}. FT-IR spectra were recorded in the range of 400−4000 cm^{-1} on a Bruker Vector22 FT-IR spectrophotometer using KBr pellets. Powder X-ray diffraction (PXRD) measurements were performed on a Bruker D8 Advance X-ray diffractometer using Cu Kα radiation (λ = 1.5418 Å), in which the X-ray tube was operated at 40 kV and 40 mA. Details of the crystal parameters, data collection, and refinements for the complex are summarized in Table S1, and selected bond lengths and angles are listed in Table S2.

Synthesis of $[Cu_3(L)_2(pyz)(H_2O)]\cdot 13DMF$ (1). A mixture of $Cu(NO_3)_2\cdot 3H_2O$ (72.4 mg, 3 mmol), H_3L (72.5 mg, 2 mmol), pyz (80.0 mg, 10 mmol), DMF (10 mL) was treated by ultrasonic vibration and then sealed into a Teflon-lined stainless steel container and heated at 140 ℃ for 72 hours. After cooling to room temperature, green block crystals were obtained in 95% yield (based on H_3L). Anal. Calcd for $C_{85}H_{119}N_{15}O_{26}Cu_3$: C, 52.15; H, 6.13; N, 10.73. Found: C, 52.11; H, 6.16; N, 10.80. IR (KBr pellet, cm^{-1}): 3421 (m), 2929 (m), 1671 (s), 1616 (s), 1558 (w), 1507 (w), 1389 (s), 1254 (m), 1183(w), 1094(w), 1015 (w), 862 (w), 810 (w), 780 (m), 752 (m), 711 (w), 660(m), 509 (m).

Synthesis of $[Cu_3(L)_2(2,5\text{-}Me_2pyz)(H_2O)]\cdot 12DMF$ (2). A mixture of $Cu(NO_3)_2\cdot 3H_2O$ (72.4 mg, 3 mmol), H_3L (72.5 mg, 2 mmol), 2,5-Me_2pyz (108 mg, 10 mmol), DMF (10 mL) was treated by ultrasonic vibration and then sealed into a Teflon-lined stainless steel container and heated at 140 ℃ for 72 hours. After cooling to room temperature, green block crystals were obtained in 56% yield (based on H_3L). Anal. Calcd for $C_{84}H_{116}N_{14}O_{25}Cu_3$: C, 52.75; H, 6.11; N, 10.25. Found: C, 52.65; H, 6.14; N, 10.20. IR (KBr pellet, cm^{-1}): 3427 (m), 2925 (m), 1715(m), 1656 (s), 1598 (s), 1542 (s), 1398 (vs), 1251 (w), 1179(w), 1102(w), 1052(w), 1010(w), 859 (w), 776 (m), 704(w), 505 (m).

Synthesis of $[Cu_3(L)_2(qx)(H_2O)]\cdot 12DMF$ (3). A mixture of $Cu(NO_3)_2\cdot 3H_2O$ (72.4 mg, 3 mmol), H_3L (72.5 mg, 2 mmol), qx (130.0mg, 10 mmol), DMF (10 mL) was treated by ultrasonic vibration and then sealed into a Teflon-lined stainless steel container and heated at 140 ℃ for 72 hours. After cooling to room temperature, green block crystals were obtained in 45% yield (based on H_3L). Anal. Calcd for $C_{86}H_{114}N_{14}O_{25}Cu_3$: C, 53.39; H, 5.94; N, 10.14.

Found: C, 53.35; H, 5.94; N, 10.12. IR (KBr pellet, cm^{-1}): 3401 (s), 2927 (w), 1656(s), 1610 (s), 1544(s), 1387 (vs), 1253(m), 1181 (w), 1095 (m), 1016(w), 859 (m), 777 (m), 752 (m), 709(m), 662 (m), 508(m).

Synthesis of $[Cu_3(L)_2(H_2O)_2(H_2O)]\cdot 12DMF$ (4). A mixture of $Cu(NO_3)_2\ 3H_2O$ (72.4 mg, 3 mmol), H_3L (72.5 mg, 2 mmol) and DMF (10 mL) was treated by ultrasonic vibration and then sealed into a Teflon-lined stainless steel container and heated at 140 ℃ for 72 hours. After cooling to room temperature, green block crystals were obtained in 54% yield (based on H_3L). Anal. Calcd for $C_{78}H_{116}N_{12}O_{29}Cu_3$: C, 49.93; H, 6.23; N, 8.96. Found: C, 49.95; H, 6.24; N, 8.90. IR (KBr pellet, cm^{-1}): 3401 (m), 2932 (m), 1655 (s), 1609 (s), 1542 (w), 1388 (s), 1253 (m), 1181(w), 1099(w), 1015 (w), 859 (w), 777 (m), 748 (m), 699 (w), 662(m), 489 (m).

Synthesis of $[Cu_3(L)_2(2,5\text{-}(C_3H_5O_2)_2\text{-pyz})(H_2O)]\cdot 8DMF$ (5). (2,5-$(C_3H_5O_2)_2$-pyz) (224.0 mg, 10 mmol), DMF (10 mL) and **1** (200.0 mg, 1 mmol) were mixed and then sealed into a Teflon-lined stainless steel container. It gradually increases the temperature at the rate of 10 ℃ per hour until 50 ℃. Then it retains 6 hours. The crystal is washed with fresh DMF and mixed with 2,5-$(C_3H_5O_2)_2$-pyz (200.0mg, 10 mmol) again. After cooling to room temperature, dark green block crystals were obtained in 98% yield (based on complex **1**). Anal. Calcd for $C_{76}H_{92}N_{10}O_{25}Cu_3$: C, 52.57; H, 5.34; N, 8.07. Found: C, 52.77; H, 5.44; N, 8.080. IR (KBr pellet, cm^{-1}): 3402 (s), 2928 (w), 1748(m), 1675 (s), 1614 (m), 1557 (m), 1388 (s), 1254(m), 1091 (m), 1060(w), 861 (m), 810(w), 779 (m), 751 (m), 710(m), 658 (m), 503(m).

Synthesis of $[Cu_3(L)_2(2\text{-}NH_2\text{-pyz})(H_2O)]\cdot 12DMF$ (6). NH_2-pyz (95.0mg, 10 mmol), DMF (10 mL) and **1** (200.0 mg, 1 mmol) were mixed and then sealed into a Teflon-lined stainless steel container. It gradually increases the temperature at the rate of 10 ℃ per hour until 120 ℃. Then it retains 6 hours. After cooling to room temperature, light-green block crystals were obtained in 98% yield (based on complex **1**). Anal. Calcd for $C_{164}H_{226}N_{30}O_{50}Cu_6$: C, 51.85; H, 6.00; N, 11.06. Found: C, 51.75; H, 6.04; N, 11.08. IR (KBr pellet, cm^{-1}): 3421 (s), 2931 (w), 1669 (s), 1618 (m), 1542 (m), 1438 (m), 1389 (s), 1318 (m), 1255(m), 1183 (w), 1097 (m), 1016(w), 863 (m), 811(w), 781 (m), 753 (m), 712(m), 661 (m), 514 (m).

Sample activation. Solvent-exchanged samples were obtained by immersing the as-synthesized samples in the exchange solvents for 3 days, the solvent was decanted every 8 h, and fresh solvent was added. The completely activated samples were obtained by heating the solvent-exchanged sample at 423 K under a dynamic high vacuum for 4 h.

Sorption measurements. Nitrogen (N_2) and carbon dioxide (CO_2) sorption measurements were carried out on a Belsorp-max volumetric gas sorption instrument using high purity (99.999%) gases.

X-ray crystallography. The diffraction data of **1 - 6** were collected on a Bruker Smart Apex DUO CCD with graphite-monochromated Mo Kα radiation (λ = 0.71073 Å) at 293 (2) K. The structures were solved by direct methods and refined with the full-matrix least-squares technique using the SHELXS-2014 and SHELXL-2014 programs, respectively.[3] Because the guest solvent molecules are highly disordered and impossible to refine using conventional discrete-atom models, the SQUEEZE subroutine of the PLATON software suite[4] was applied to remove the scattering from the highly disordered solvent molecules, and sets of solvent-free diffraction intensities were produced. The final formula was calculated from the SQUEEZE results, TGA, and elemental analysis. Non-hydrogen atoms were refined anisotropically. The large thermal parameters of atoms from pyz derivatives are caused by disorder of the atoms. All hydrogen atoms were generated geometrically except hydrogen from coordinated water, which was located directly.

Recyclability of catalysts. At the end of Knoevenagel condensation catalytic reaction, the catalyst was isolated from the reaction solution, dried at room temperature, and then reused in the second run of the reaction. The initial activity of the catalyst was also obtained in the second run, showing that the framework of the catalyst remains intact during the catalytic cycles. The catalyst remained effective for up to 3 cycles for reactions (Figure S5). The catalyst used in the second run was also analyzed by XRD, but no significant change was observed.

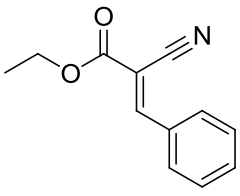

(*E*)-ethyl 2-cyano-3-phenylacrylate ^{1}H NMR spectrum (400MHz, DMSO-d_6, ppm) δ = 8.37 (s, 1H); 8.04 (d, *J* = 7.5 Hz, 2H), 7.63 - 7.55 (m, 3H); 4.31 (q, *J* = 7.1 Hz, 2H); 1.30 (t, *J* = 7.1 Hz, 3H).

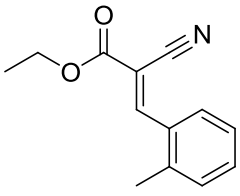

(*E*)-ethyl 2-cyano-3-o-tolylacrylate ^{1}H NMR spectrum (400MHz, DMSO-d_6, ppm) δ = 8.57 (s, 1H); 7.51(d, *J* = 7.1 Hz, 1H); 7.39(m, 3H);4.36 (q, *J* = 7.1 Hz, 2H); 2.42 (s, 3H); 1.35 (t, *J* = 7.1 Hz, 3H).

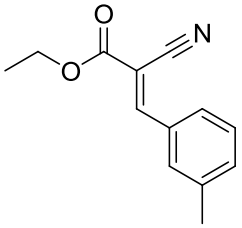

(*E*)-ethyl 2-cyano-3-m-tolylacrylate ^{1}H NMR spectrum (400MHz, DMSO-d_6, ppm) δ = 8.36 (s, 1H); 7.90(d, *J* = 7.8 Hz, 1H); 7.50(m, 3H); 4.36 (q, *J* = 7.0 Hz, 2H); 2.41 (s, 3H); 1.32 (t, *J* = 7.1 Hz, 3H).

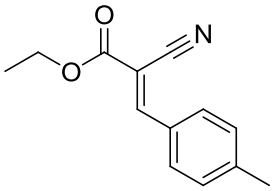

(*E*)-ethyl 2-cyano-3-p-tolylacrylate ^{1}H NMR spectrum (400MHz, DMSO-d_6, ppm) δ = 8.35(s, 1H); 7.99(d, *J* = 7.6 Hz, 2H); 7.41(d, *J* = 7.6 Hz, 2H); 4.36 (q, *J* = 7.1 Hz, 2H); 2.41 (s, 3H); 1.32 (t, *J* = 7.1 Hz, 3H).

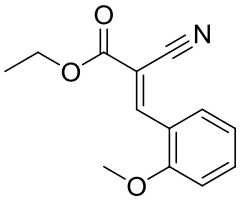

(*E*)-ethyl 2-cyano-3-(2-methoxyphenyl)acrylate ^{1}H NMR spectrum (400MHz, DMSO-d_6, ppm) δ = 8.61(s, 1H); 7.66(d, *J* = 7.3 Hz, 2H); 7.21 ~ 7.04(m, 3H); 4.32 (q, *J* = 7.0 Hz, 2H); 3.92 (s, 3H); 1.32 (t, *J* = 7.0 Hz, 3H).

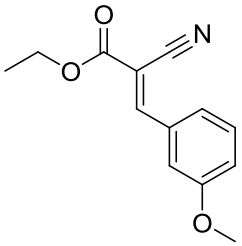

(*E*)-ethyl 2-cyano-3-(3-methoxyphenyl)acrylate ^{1}H NMR spectrum (400MHz, DMSO-d_6, ppm) δ = 8.48(s, 1H); 7.65(q, *J* = 6.3 Hz, 1H); 7.53 (m, 2H); 7.26 ~ 7.01(m, 1H); 4.32 (q, *J* = 7.3 Hz, 2H); 3.82 (s, 3H); 1.32 (t, *J* = 7.3 Hz, 3H).

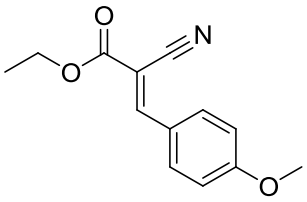

(*E*)-ethyl 2-cyano-3-(4-methoxyphenyl)acrylate ^{1}H NMR spectrum (400MHz, DMSO-d_6, ppm) δ = 8.33(s, 1H); 8.11(d, *J* = 6.3 Hz, 2H); 7.17 (d, *J* = 8.9 Hz, 2H); 4.33 (q, *J* = 7.1 Hz, 2H); 3.88 (s, 3H); 1.32 (t, *J* = 7.1 Hz, 3H)

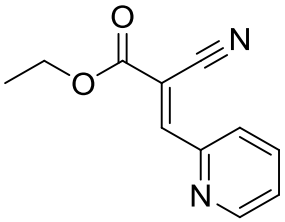

(*E*)-ethyl 2-cyano-3-(pyridin-2-yl)acrylate

^{1}H NMR (400MHz, $CDCl_3$, ppm) δ = 8.65-8.92 (m, 2H); 8.19 (s, 1H); 7.75 (d, *J* = 5.1 Hz 2H); 4.41 (q, *J* = 7.0 Hz, 2H); 1.41 (t, *J* = 7.0 Hz, 3H),

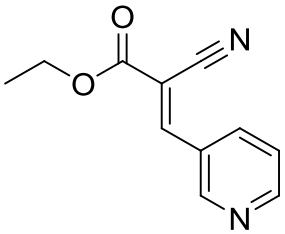

(*E*)-ethyl 2-cyano-3-(pyridin-3-yl)acrylate

^{1}H NMR (400MHz, $CDCl_3$, ppm) δ = 8.91 (s,1H); 8.74 (d, J = 2.74 Hz, 1H); 8.57 (d, J = 7.8Hz, 1H); 8.25 (s, 1H); 7.47 (t, *J* = 6.6 Hz, 1H); 4.39 (q, J = 7.0 Hz, 2H); 1.40 (t, *J* = 7.0 Hz, 3H)

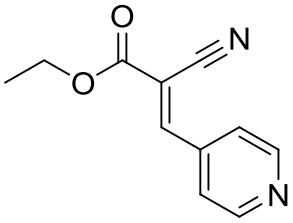

^{1}H NMR (400MHz, $CDCl_3$, ppm) δ = 8.65-8.92 (m, 2H); 8.19 (s, 1H); 7.75 (d, *J* = 5.1 Hz 2H); 4.41 (q, *J* = 7.0 Hz, 2H); 1.41 (t, *J* = 7.0 Hz, 3H).

Supplementary references:

(1) J. K. Schnobrich, O. Lebel, K. A. Cychosz, A. Dailly, A. G. Wong-Foy and A. J. Matzger, *J. Am. Chem. Soc.*, 2010, **132**, 13941.

(2) S. K. Das and J. Frey, *Tetrahedron Lett.*, 2012, **53**, 3869.

(3) a) G. M. Sheldrick, SHELXS-2014, Program for the Crystal Structure Solution, University of Göttingen, Göttingen, Germany, **2014**; b) G. M. Sheldrick, SHELXL-2014, Program for the Crystal Structure Solution, University of Göttingen, Göttingen, Germany, **2014**.

(4) Spek, A.L. (2009). Acta Cryst. D65, 148-155.